

# The Geometry of Linear Program Compression: An Exact Characterization and Learning Algorithm

Yuhan Ye  
MIT  
yyh03@mit.edu

Omar Bennouna  
MIT  
omarben@mit.edu

## Abstract

We study how much a linear program (LP) can be compressed when solved repeatedly, given prior knowledge about its objective function. Existing data-driven projection methods learn low-dimensional surrogate LPs with approximate objective-value guarantees, but cannot provably identify the optimal projection for a prescribed compression budget. We instead ask a sharper question: how far can an LP be compressed into a lower-dimensional equivalent while *exactly* preserving optimality, enabling faster repeated solves with no loss in solution quality? We provide an exact geometric characterization of such compressed LPs, together with a tractable sample-based learning algorithm that comes with fast-rate guarantees: the compressed LP recovers the optimal solution of an unseen instance with probability at least  $1 - \tilde{O}(d^*/n)$ , where  $d^*$  is the dimension of the decision-relevant subspace, and  $n$  is the number of available historical LP samples. This  $1/n$  dependence is sharper than the  $\tilde{O}(1/\sqrt{n})$  uniform-convergence rates of approximate projection methods. Our framework further exposes a tunable tradeoff between the dimension of the compressed LP and the probability of recovering the optimal solution, allowing the user to trade compression for accuracy.

## 1 Introduction

Many decision systems repeatedly solve linear programs (LPs) over the same feasible region while the objective changes. This setting arises in routing, resource allocation, network operations, and other large-scale planning tasks. In such applications, one would like to compress the repeated optimization problem once and reuse the compressed representation on future instances. Projection-based approaches address this goal by learning or sampling a low-dimensional projection and solving a surrogate LP in the projected space (Sakaue and Oki, 2024; Iwata and Sakaue, 2025), or sampling random projections Vu et al. (2018). These methods can yield substantial speedups, but their guarantees are typically approximate, lack interpretability and exact optimality guarantees.

We study the exact version of this compression problem. Let

$$\min_{x \in \mathcal{X}} c^\top x \tag{1}$$

be a family of LPs with a fixed nonempty bounded polytope  $\mathcal{X} \subseteq \mathbb{R}^d$  and a cost vector  $c$  known to lie in a prior set  $\mathcal{C} \subseteq \mathbb{R}^d$ . The central question we propose is:

When an LP is solved repeatedly with varying costs, how much can future instances be reduced in dimension while exactly preserving optimality, given prior knowledge about the cost vector?

Here, prior knowledge takes the form of either a set  $\mathcal{C} \subset \mathbb{R}^d$  containing the cost vector, historical samples of  $c$ , or both. We first focus on the known-prior-set setting and later extend our results to the case where only historical samples are available. These models arise in many real-world problems. In transportation planning for example, fastest-route problems can be written as shortest path or min-cost flow LPs: the network is fixed, while edge travel times fluctuate locally. In contextual linear optimization, costs are generated from context and are naturally modeled as supported on a bounded set. In such settings, exact optimality-preserving compression can speed up repeated LP solves and reduce the amount of information that must be learned about  $c$ .

Against this background, we show throughout the paper that the quantity governing LP compression is not the ambient dimension  $d$ , but the dimension of the *decision-relevant subspace*: the subspace spanned by directions along which perturbations to  $c$  can change the optimal solution. Crucially, even when  $d$  is very large, this subspace can be low-dimensional. Building on [Bennouna et al. \(2025\)](#) and [Bennouna et al. \(2026\)](#), when  $\mathcal{C}$  is convex and open, this subspace can be written as

$$\text{dir}(\mathcal{X}^*(\mathcal{C})) := \text{span}\{x - x' : x, x' \in \mathcal{X}^*(\mathcal{C})\},$$

where  $\mathcal{X}^*(\mathcal{C})$  denotes the set of all optimal solutions as  $c$  varies over  $\mathcal{C}$ . Equivalently,  $\text{dir}(\mathcal{X}^*(\mathcal{C}))$  is the span of differences between reachable optimal solutions. Important insight from their results is the following: a set of function evaluations  $c^\top q_1, \dots, c^\top q_r$  contains the necessary information to recover the solution set of (1) if and only if  $\text{dir}(\mathcal{X}^*(\mathcal{C})) \subseteq \text{span}(q_1, \dots, q_r)$ ; such a set  $\{q_1, \dots, q_r\}$  is called a *sufficient decision dataset* (SDD). The key implication is that the optimal solution depends on  $c$  only through its projection onto  $\text{dir}(\mathcal{X}^*(\mathcal{C}))$ , and  $\text{dir}(\mathcal{X}^*(\mathcal{C}))$  itself is the smallest subspace with this property.

Recent work by [Ye et al. \(2026\)](#), clarifies the computational and statistical landscape of this characterization. On the negative side, constructing a basis of the decision-relevant space  $\text{dir}(\mathcal{X}^*(\mathcal{C}))$  is NP-hard and coNP-hard. On the positive side, the same work shows that one can learn such a basis from i.i.d. cost vector samples. In particular, they provide an algorithm that outputs a set of vectors  $\{q_1, \dots, q_r\}$  such that for any unobserved instance  $c \in \mathcal{C}$ , the measurements  $c^\top q_1, \dots, c^\top q_r$  have enough information to solve (1) with probability at least  $1 - \tilde{O}(d^*/n)$  where  $n$  is the sample size and  $d^* := \dim \text{dir}(\mathcal{X}^*(\mathcal{C}))$ .

From the standpoint of LP compression, three challenges remain. First, the existing SDD literature ([Bennouna et al., 2025, 2026](#)) characterizes which measurements suffice to recover optimal decisions, but it does not provide compressed reformulations of LPs induced by the decision-relevant subspace. Second, the sample-based guarantee for the algorithm in [Ye et al. \(2026\)](#) assumes a strong nondegeneracy condition, whereas many repeated-LP models of practical interest are degenerate. Third, although it is relevant in practice to assume that  $\mathcal{C}$  is known, one may only observe historical cost samples without knowing an exact prior set in data-driven settings.

## 1.1 Our contributions

1. **Exact reduced LPs with a fast-rate learning certificate.** We turn the decision-relevant subspace characterization of [Bennouna et al. \(2025, 2026\)](#) into an explicit solver-side reduction: any subspace containing  $\text{dir}(\mathcal{X}^*(\mathcal{C}))$  yields an exact reduced LP, and a basis of  $\text{dir}(\mathcal{X}^*(\mathcal{C}))$  gives a minimal exact  $d^*$ -variable reformulation. Unlike approximate projection methods, which treat the projection as a black-box parameter to be optimized without identifying what makes it optimal, our framework reveals  $\text{dir}(\mathcal{X}^*(\mathcal{C}))$  as the unique object that governs exact compression, and as opposed to random projection and projection learning methods, can be applied to totally unimodular LPs. When sufficient power is available, this reduction requires no data at all; when it is not, cost samples suffice with provable guarantees of recovering the optimal solution on

any future instance with probability at least  $1 - \tilde{O}(d^*/n)$ , a  $1/n$  rate that is sharper than the  $\tilde{O}(1/\sqrt{n})$  rates of approximate methods. In contrast with the learner of [Ye et al. \(2026\)](#), our approach does not require a nondegeneracy assumption on the LP.

2. **Sample-based learning under unknown priors.** We extend our framework to the setting where the uncertainty set  $\mathcal{C}$  is unknown, giving an iterative algorithm that progressively recovers the decision-relevant subspace one new direction at a time from training samples. The resulting compression enjoys fast-rate generalization guarantees and outperforms both projection-learning methods and random projections. We further extend our approach to expose a tunable tradeoff between compression and optimality: by selectively incorporating training samples into the learning process, the user can shrink the compressed LP at a controlled cost in optimal-solution recovery.
3. **Empirical separation from approximate projections.** We compare our exact reduction algorithm against projection learning baselines on both synthetic repeated-LP families and standard Netlib benchmark instances. We show that our exact reduction substantially outperforms all baselines in terms of data requirement and accuracy.

## 1.2 Related work

**Decision-sufficient representations for linear programs.** [Bennouna et al. \(2025\)](#) and [Bennouna et al. \(2026\)](#) characterize what information about the cost vector is needed to recover optimal decisions. Their key finding is that optimality is governed by a single geometric object, the subspace  $\text{dir}(\mathcal{X}^*(\mathcal{C}))$  spanned by differences between reachable optimal solutions: a set of linear measurements  $\{c^\top q_1, \dots, c^\top q_r\}$  is sufficient to solve (1) if and only if the directions  $\{q_1, \dots, q_r\}$  span  $\text{dir}(\mathcal{X}^*(\mathcal{C}))$ . [Ye et al. \(2026\)](#) move to the data-driven setting, where the cost vector is random but samples are available, and show that directions in  $\text{dir}(\mathcal{X}^*(\mathcal{C}))$  can be learned incrementally from cost samples with provable out-of-sample guarantees. Our work builds on this line of research but shifts the focus from information-theoretic sufficiency to optimization: we ask what a known  $\text{dir}(\mathcal{X}^*(\mathcal{C}))$  buys on the solver side, how to learn it under weaker geometric assumptions, and how to calibrate a high-coverage working prior when the prior set  $\mathcal{C}$  is unknown.

**Parametric and multiparametric optimization.** Repeated optimization with varying parameters has long been studied through parametric programming and sensitivity analysis ([Fiacco, 1983](#)). In control and explicit model predictive control, a classical strategy is to precompute the full piecewise-affine solution map offline through multiparametric programming ([Bemporad et al., 2002](#); [Alessio and Bemporad, 2009](#); [Borrelli et al., 2017](#)). These methods target an explicit representation of the optimizer over a parameter region. Our goal is different: we do not attempt to tabulate the entire solution map, but rather to identify the task-dependent subspace of cost directions that can change the optimizer and to use it for exact low-dimensional reformulation.

**Approximate projections for repeated LPs.** Classical projection methods reduce LP size approximately, either through random projections or other dimension-reduction primitives that preserve feasibility and objective values only approximately ([Vu et al., 2018](#); [Poirion et al., 2023](#); [d’Ambrosio et al., 2020](#)). [Sakaue and Oki \(2024\)](#) study shared data-driven projections for repeated LPs and analyze them through pseudo-dimension bounds, while [Iwata and Sakaue \(2025\)](#) learn instance-specific projections for heterogeneous LP families. Related extensions now also exist beyond LPs, for example in quadratic programming ([Nguyen and Nguyen, 2026](#)). It is, however, unclear whether LP solutions produced by projection approaches correspond to feasible combinatorial

solutions for problems represented through LP relaxations, such as shortest path problems, because recovered solutions are not guaranteed to be extreme points or integral for the original LP instance. Our method provably recovers optimal extreme points of the original LP.

**Learning to accelerate optimization.** A broader recent literature uses data to accelerate future solves without explicitly learning a decision-sufficient subspace. Representative directions include learning warm starts for iterative solvers (Sambharya et al., 2024), predicting active sets or optimization strategies (Bertsimas and Stellato, 2021; Misra et al., 2022), and amortized optimization methods that map instances directly to approximate solutions (Amos, 2023; Chen et al., 2022). These approaches can substantially reduce computation, but they typically do not identify a task-dependent exact low-dimensional LP together with a sufficiency guarantee.

**Data-driven algorithm design and generalization guarantees.** Gupta and Roughgarden (2017), Gupta and Roughgarden (2020), Balcan et al. (2017), Balcan (2021), and Balcan et al. (2024) formalize the broader viewpoint that one can learn algorithmic components from representative instances and still obtain out-of-sample guarantees. The LP-projection works above fit this template, with sample complexity bounds obtained via uniform-convergence arguments based on pseudo-dimension. Our framework departs from this approach in two ways. First, the object being learned is different: instead of a generic projection matrix, we learn a specific geometric object, the decision-relevant subspace, and our algorithm grows this subspace one direction at a time, only when a training sample exposes a direction the current subspace misses. Second, the proof technique is different: this incremental structure makes our learner a *stable compression scheme* in the sense of Hanneke and Kontorovich (2021), which yields a fast  $\tilde{O}(d^*/n)$  rate instead of the slower  $\tilde{O}(1/\sqrt{n})$  rate produced by uniform-convergence arguments. A similar gain appears in predict-then-optimize, where sample complexity scales with the dimension of the induced decision class rather than the ambient cost dimension (El Balghiti et al., 2023); we exploit the same idea to cleanly separate the samples spent on calibrating the working prior from the samples spent on discovering decision-relevant directions.

## 2 Preliminaries

We consider the polyhedral LP

$$\min_{x \in \mathcal{X}} c^\top x, \quad \mathcal{X} := \{x \in \mathbb{R}^d : Ax \leq b\}, \quad (2)$$

where  $\mathcal{X}$  is nonempty and bounded and the cost vector  $c$  lies in a convex prior set  $\mathcal{C} \subseteq \mathbb{R}^d$ . We denote  $\mathcal{X}^\angle$  as the set of extreme points of  $\mathcal{X}$ . For  $c \in \mathbb{R}^d$ , set  $\mathcal{X}^*(c) := \arg \min_{x \in \mathcal{X}} c^\top x$  and  $\mathcal{X}^*(\mathcal{C}) := \bigcup_{c \in \mathcal{C}} \mathcal{X}^*(c)$ . Following Bennouna et al. (2025),  $\mathcal{D} := \{q_1, \dots, q_r\} \subset \mathbb{R}^d$  is a sufficient decision dataset (SDD) for  $(\mathcal{X}, \mathcal{C})$  if for any  $c \in \mathcal{C}$  the observation of the evaluations  $c^\top q_1, \dots, c^\top q_r$  can be mapped to the solution set  $\arg \min_{x \in \mathcal{X}} c^\top x$ , i.e. they contain sufficient information to find the solution to (1). Bennouna et al. (2025) argue that the quantity of interest that determines the information required to solve (1) is the decision relevant space  $\text{dir}(\mathcal{X}^*(\mathcal{C}))$ , which is equal to the span of all directions along which reachable optimal solutions can differ. In particular, they provide the following exact characterization.

**Theorem 1.** *Assume  $\mathcal{C}$  is open and convex. A finite dataset  $\mathcal{D} \subseteq \mathbb{R}^d$  is an SDD for  $(\mathcal{X}, \mathcal{C})$  if and only if  $\text{dir}(\mathcal{X}^*(\mathcal{C})) \subseteq \text{span}(\mathcal{D})$ . In particular, the minimum cardinality of an SDD is  $d^* := \dim \text{dir}(\mathcal{X}^*(\mathcal{C}))$ .*

This characterization has consequences not only from an experimental design perspective, but also for the computational speedup of LPs. In particular, we show that any sufficient dataset yields a reformulation of (1) whose dimension equals the size of the dataset. The question we address can be stated rigorously as follows: given an LP of the form (1) with a random cost vector  $c$ , and given either an uncertainty set for  $c$  or samples from its distribution, how can we construct a lower-dimensional LP of the form

$$\min_{y \in \mathcal{X}'} c'^{\top} y, \quad (3)$$

where  $c'$  and  $\mathcal{X}'$  are built from  $c$  and  $\mathcal{X}$ , such that  $y$  can be mapped to a solution of (1) with high probability?

We show that both settings, samples from the distribution of  $c$  and an uncertainty set for  $c$ , can be handled within the same framework by reducing the former to the latter. The key step in obtaining a lower-dimensional reformulation of (1) is to construct a sufficient dataset from the data. Two approaches are available. If an uncertainty set is available and the LP instance is of moderate size or sufficient computational power is available, [Bennouna et al. \(2025\)](#) formulate a mixed-integer program (MIP) that iteratively constructs a sufficient dataset. When the instance is too large for an MIP to be tractable, and data is available, we instead process cost samples sequentially, learning a new decision relevant direction only when the current dataset fails to recover the optimal solution at the incoming sample; the dataset therefore grows only on informative samples and never exceeds  $d^*$  directions.

### 3 Exact LP Compression via Sufficient-Decision Subspaces

#### 3.1 Exact reduction from a sufficient-decision subspace

The characterization in Theorem 1 identifies which cost measurements are sufficient for recovering optimal decisions. We now use the same geometry on the solver side: once a subspace contains the decision-relevant directions, the original LP can be solved exactly on a lower-dimensional affine slice. Proofs and further details of this section are deferred to Section A.1.

Fix a prior set  $\mathcal{C}$  containing the possible cost vectors. We call an affine subspace  $V \subseteq \mathbb{R}^d$  *exact-sketching* if it preserves the full optimizer set on the prior, namely, for every  $c \in \mathcal{C}$ ,

$$\arg \min_{x \in \mathcal{X} \cap V} c^{\top} x = \arg \min_{x \in \mathcal{X}} c^{\top} x.$$

**Theorem 2** (Exact LP reduction from a sufficient-decision subspace). *An affine subspace  $V \subseteq \mathbb{R}^d$  is exact-sketching on  $\mathcal{C}$  if and only if*

$$\text{dir}(\mathcal{X}^*(\mathcal{C})) \subseteq \text{dir}(V) \quad \text{and} \quad V \cap \mathcal{X}^*(\mathcal{C}) \neq \emptyset.$$

We next show how an exact-sketching affine subspace yields a potentially lower-dimensional reformulation of Equation (1). Fix an anchor  $x_0 \in \mathcal{X}$  and a matrix  $U \in \mathbb{R}^{d \times r}$  with linearly independent columns. Let  $T_{U, x_0}(z) := x_0 + Uz$ , let  $\mathcal{Z}_{U, x_0} := \{z \in \mathbb{R}^r : T_{U, x_0}(z) \in \mathcal{X}\}$  be the compressed feasible region<sup>1</sup>, and let  $F_{U, x_0}(c) := \arg \min_{z \in \mathcal{Z}_{U, x_0}} (U^{\top} c)^{\top} z$  be the compressed optimizer set. If  $x_0 \in \mathcal{X}^*(\mathcal{C})$  and  $\text{range}(U) \supseteq \text{dir}(\mathcal{X}^*(\mathcal{C}))$ , then Theorem 2 applies to the affine space  $x_0 + \text{range}(U)$ , and the following optimizer-set identity stands for every  $c \in \mathcal{C}$ :

$$\mathcal{X}^*(c) = T_{U, x_0}(F_{U, x_0}(c)). \quad (\text{Exact}(U, x_0, c))$$

<sup>1</sup>In the polyhedral model  $\mathcal{X} = \{x \in \mathbb{R}^d : Ax \leq b\}$ ,  $\mathcal{Z}_{U, x_0} = \{z \in \mathbb{R}^r : A(x_0 + Uz) \leq b\}$ .

Moreover,

$$\min_{x \in \mathcal{X}} c^\top x = c^\top x_0 + \min_{z \in \mathcal{Z}_{U,x_0}} (U^\top c)^\top z. \quad (4)$$

Thus solving the  $r$ -variable LP in (4) and lifting by  $T_{U,x_0}$  recovers an optimal solution of the original LP instance. To guarantee  $\text{Exact}(U, x_0, c)$  stands for every  $c \in \mathcal{C}$ , the minimal choice  $\text{range}(U) = \text{dir}(\mathcal{X}^*(\mathcal{C}))$  gives an exact  $d^*$ -variable affine reformulation. This however can be both NP and coNP-hard (Ye et al., 2026), even though it can be done using the MIP formulation in Bennouna et al. (2026). Our approach aims to find  $U$  such that  $\text{Exact}(U, x_0, c)$  holds with high probability under the distribution of  $c$ . This allows us to design a tractable algorithm to do so.

The next result further shows that vertex optimizers are preserved if  $\text{Exact}(U, x_0, c)$  holds, which is useful in real-world applications.

**Corollary 3** (Vertex optimizers are preserved). *If  $\text{Exact}(U, x_0, c)$  holds, then*

$$T_{U,x_0} \left( F_{U,x_0}(c) \cap \mathcal{Z}_{U,x_0}^\angle \right) = \mathcal{X}^*(c) \cap \mathcal{X}^\angle.$$

Thus, if a reduced LP solver returns a vertex optimizer in  $\mathcal{Z}_{U,x_0}$  under the exactness event  $\text{Exact}(U, x_0, c)$ , its lift is a vertex optimizer of the original LP. This is useful for combinatorial problems. For example, shortest path, min-cost flow, and assignment problems admit LP formulations with totally unimodular constraints, so lifting a reduced vertex optimizer yields an integral optimal solution of the original problem.

**Comparison with homogeneous linear projection reductions.** Projection-based LP reductions such as Sakaue and Oki (2024) choose a projection matrix  $P \in \mathbb{R}^{d \times k}$  and substitute  $x = Py$ , restricting the feasible set to the linear slice  $\mathcal{X} \cap \text{range}(P)$  through the origin. Our reduction instead uses an *affine* slice  $\mathcal{X} \cap (x_0 + \text{range}(U))$  anchored at a reachable optimal point  $x_0 \in \mathcal{X}^*(\mathcal{C})$ . This difference matters in two ways. First, we know exactly how to choose the slice: setting  $\text{range}(U) = \text{dir}(\mathcal{X}^*(\mathcal{C}))$  yields an exact and minimal reformulation in  $d^*$  variables. Projection methods, by contrast, optimize  $P$  heuristically and offer no characterization of which  $k$ -dimensional subspace is sufficient, nor any guarantee that their learned  $P$  recovers a sufficient one. Second, even an optimally chosen linear subspace would need one additional variable: the smallest linear subspace containing  $x_0 + \text{dir}(\mathcal{X}^*(\mathcal{C}))$  is  $\text{span}\{x_0\} + \text{dir}(\mathcal{X}^*(\mathcal{C}))$ , whose dimension can be as large as  $d^* + 1$ . A homogeneous projection therefore spends an extra dimension just to encode the anchor offset, which the affine formulation handles for free. Example 4 illustrates this gap.

**Example 4** (Affine compression can beat homogeneous projection). *Let  $\mathcal{X} = [-1, 1]^2$  and  $\mathcal{C}_\rho = (-1 - \rho, -1) \times (-1, 1)$  for  $\rho > 0$ . Since every  $c \in \mathcal{C}_\rho$  has  $c_1 < 0$ , all optimizers lie on the right edge:  $\mathcal{X}^*(\mathcal{C}_\rho) = \{1\} \times [-1, 1]$  and  $\text{dir}(\mathcal{X}^*(\mathcal{C}_\rho)) = \text{span}\{(0, 1)\}$ . Thus the anchored line  $x = (1, 0) + z(0, 1)$ ,  $z \in [-1, 1]$ , is an exact one-variable reduction. In contrast, a one-dimensional homogeneous slice through the origin cannot contain the full right edge; if  $c$  is uniform on  $\mathcal{C}_\rho$ , every such slice incurs expected objective gap at least  $1/2$  (verified in Section A.1).*

### 3.2 Learning exact compression from samples

We now describe the sample-based learning algorithm (Algorithm 1). It maintains a matrix  $U$  of decision-relevant directions discovered so far; together with a fixed anchor  $x_0 \in \mathcal{X}^*(\mathcal{C})$ , obtained by picking any  $c_0 \in \mathcal{C}$  and taking  $x_0 \in \mathcal{X}^*(c_0)$ , it defines the candidate compressed feasible region  $x_0 + \text{range}(U)$ . Training costs  $c_1, \dots, c_n$  are processed one at a time, and  $U$  grows whenever a new

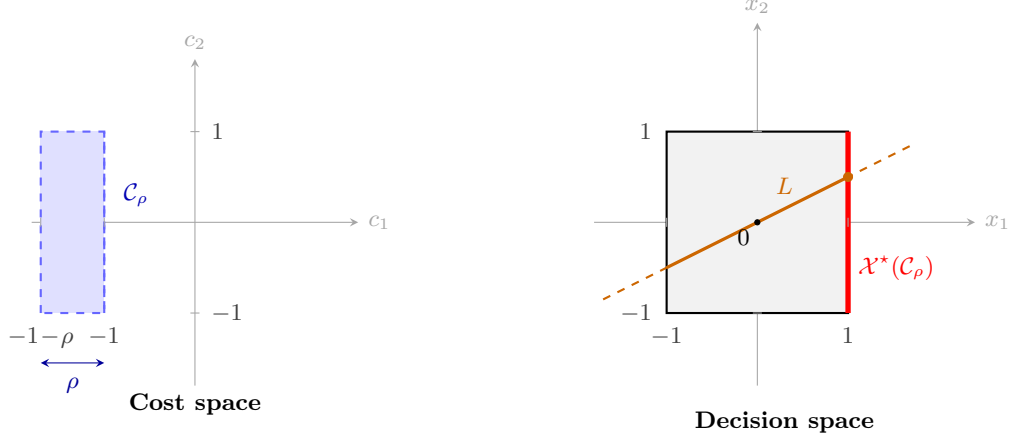


Figure 1: Affine exact compression versus a homogeneous one-dimensional slice.

---

**Algorithm 1** Sample-based learning algorithm

---

**Require:** Feasible polytope  $\mathcal{X}$ , fixed reachable anchor  $x_0 \in \mathcal{X}^*(\mathcal{C})$ , samples  $c_1, \dots, c_n$ , and deterministic tie-breaking for all choices.

**Ensure:** A compression matrix  $U_n$  and a hard-sample index set  $T_n$ .

- 1: Initialize  $U_0 \leftarrow [] \in \mathbb{R}^{d \times 0}$  and  $T_n \leftarrow \emptyset$ .
  - 2: **for**  $i = 1, \dots, n$  **do**
  - 3:   Set  $U_i \leftarrow U_{i-1}$ .
  - 4:   **while**  $\mathcal{X}^*(c_i) \not\subseteq x_0 + \text{range}(U_i)$  **do**
  - 5:     Choose  $x \in \mathcal{X}^*(c_i) \cap \mathcal{X}^\angle$  with  $x - x_0 \notin \text{range}(U_i)$ .
  - 6:      $U_i \leftarrow [U_i \ x - x_0]$  and  $T_n \leftarrow T_n \cup \{i\}$ .
  - 7:   **end while**
  - 8: **end for**
  - 9: **return**  $U_n$  and  $T_n$ .
- 

sample reveals a direction the current slice misses. For each  $c_i$ , the algorithm checks whether the optimal face  $\mathcal{X}^*(c_i)$  is contained in the current slice  $x_0 + \text{range}(U)$ . If yes, it proceeds to  $c_{i+1}$ . If no, then since  $\mathcal{X}^*(c_i)$  is the convex hull of its vertices, some vertex  $x$  lies outside the slice; the algorithm appends  $x - x_0$  as a new column of  $U$  and rechecks. This test-and-append loop repeats until the full optimal face is contained. Samples that trigger at least one append are called *hard instances*.

**Theorem 5** (Exact-compression certificate and tractability). *Fix an anchor  $x_0 \in \mathcal{X}^*(\mathcal{C})$  independently of the  $n$  training costs. Run Algorithm 1 on  $n$  i.i.d. costs drawn from a distribution supported on  $\mathcal{C}$ . Then*

$$\text{range}(U_n) \subseteq \text{dir}(\mathcal{X}^*(\mathcal{C})), \quad |T_n| \leq \text{rank}(U_n) \leq d^*,$$

and  $\text{Exact}(U_n, x_0, c_i)$  holds for every training sample  $i = 1, \dots, n$ . Moreover, for any  $\delta \in (0, 1)$ , with probability at least  $1 - \delta$ ,

$$\mathbb{P}_{c \sim P_c}[\text{Exact}(U_n, x_0, c)] \geq 1 - \frac{4}{n}(6|T_n| + \log(e/\delta)) \geq 1 - \frac{4}{n}(6d^* + \log(e/\delta)). \quad (5)$$

Note that Algorithm 1 only requires LP solves and hence runs in polynomial time.

**Sample-free construction and the computational tradeoff.** The sample-based learner is complementary to the deterministic alternative. When  $\mathcal{C}$  is convex, [Bennouna et al. \(2025\)](#) construct the decision-relevant subspace directly from the known pair  $(\mathcal{X}, \mathcal{C})$  using an iterative mixed-integer program, requiring no cost samples and yielding a global SDD. The catch is computational: [Ye et al. \(2026\)](#) show that, for open convex  $\mathcal{C}$ , constructing a minimum-size global SDD and even computing its minimum size are NP-hard and coNP-hard. Our sample-based learner trades this combinatorial hardness for a statistical cost: each update requires only LP solves, optimal-face containment tests, and rank tests, but the algorithm needs representative cost samples to discover the relevant directions. Once the sampled directions span  $\text{dir}(\mathcal{X}^*(\mathcal{C}))$ , the compression is globally exact ([Theorem 2](#)); until then, [Theorem 5](#) bounds the probability that the current compression fails on a fresh sample.

### 3.3 Ruling out instances that are too hard

[Algorithm 1](#) does not require knowledge of  $\mathcal{C}$ . Given enough samples, the algorithm learns an exact reformulation of [\(1\)](#) for  $c$  ranging over the *entire* support of its distribution, which is often too conservative. A natural way to address this is to rule out training instances that are *too hard*, i.e. so unlikely to occur that the extra dimensions needed to handle them exactly are not worth the cost. This also allows to potentially trade optimality for LP compression by only learning the most important decision relevant directions. To do so, we construct a confidence set  $\hat{\mathcal{C}}$  from the data, and only learn the relevant decision directions for the cost vector samples that are inside the confidence set, which we define in the following.

**Definition 6** ( $(\rho, \delta_0)$ -estimated prior). *Let  $P_c$  be the cost distribution. A pilot-measurable random convex set  $\hat{\mathcal{C}} \subseteq \mathbb{R}^d$  is a  $(\rho, \delta_0)$ -estimated prior if*

$$\mathbb{P}_{\text{pilot}} \left[ P_c(c \notin \hat{\mathcal{C}}) \leq \rho \right] \geq 1 - \delta_0.$$

We can construct a convex estimated prior  $\hat{\mathcal{C}}_{\rho, \delta_0}$  satisfying [Definition 6](#); the distribution-free construction and its proof are deferred to [Section A.3.1](#).

We next state the learning guarantee for this new framework. Let  $\hat{\mathcal{C}}$  be a  $(\rho, \delta_0)$ -estimated prior independent of the representation-learning sample, and define  $\mathcal{E}_0 := \{P_c(c \notin \hat{\mathcal{C}}) \leq \rho\}$ . On  $\mathcal{E}_0$ , set  $P_{\hat{\mathcal{C}}} := P_c(\cdot \mid c \in \hat{\mathcal{C}})$  and  $\hat{d}_\star := \dim \text{dir}(\mathcal{X}^*(\hat{\mathcal{C}}))$ . Choose an anchor  $\hat{x}_0 \in \mathcal{X}^*(\hat{\mathcal{C}})$  by selecting any  $\hat{c}_0 \in \hat{\mathcal{C}}$  and solve the original LP. Run [Algorithm 1](#) with anchor  $\hat{x}_0$  on the first  $n_1$  samples that fall inside  $\hat{\mathcal{C}}$ ; conditional on the realized  $\hat{\mathcal{C}}$  and on retaining  $n_1$  samples, these retained costs are i.i.d. from  $P_{\hat{\mathcal{C}}}$ . Let  $U_{n_1}$  be the output compression matrix.

**Theorem 7** (Learning with a calibrated estimated prior). *Under the preceding setup, for any  $\delta_1 \in (0, 1)$ , with probability at least  $1 - \delta_0 - \delta_1$  over the pilot and retained representation-learning samples,*

$$\mathbb{P}_{c \sim P_c} [\text{Exact}(U_{n_1}, \hat{x}_0, c)] \geq 1 - \rho - \frac{4}{n_1} (6\hat{d}_\star + \log(e/\delta_1)). \quad (6)$$

*Consequently, taking  $\hat{\mathcal{C}} = \hat{\mathcal{C}}_{\rho, \delta_0}$  from [Proposition 13](#) gives the same distribution-free unknown-prior certificate.*

The first term,  $\rho$ , is the probability mass intentionally left outside the calibrated estimated prior, while the second term is the stable-compression risk for costs drawn from the conditional distribution inside the realized prior. The parameter  $\rho$  controls the degree to which low-probability instances are discarded: the larger  $\rho$ , the smaller the dimension  $\hat{d}_\star$  of the learned decision-relevant subspace, which would result in a more compressed LP reformulation. This lets us calibrate  $\rho$  to prioritize

optimality (small  $\rho$ ) or compression (large  $\rho$ ). In some cases, discarding rare instances costs very little in optimality while yielding substantial gains in compression, as we show in Section 4.

## 4 Numerical Experiments

We evaluate the sample-based exact-compression framework in the unknown-prior setting of Section 3.3. The learner first builds a calibrated convex working prior from historical cost samples and then learns the decision-relevant directions inside that set. The main text reports the three diagnostics that directly test this mechanism: how the dimensions of the learned exact reformulation grow with samples, how performance changes as the target outside-mass level  $\rho$  is varied, and how the calibrated exact method compares with a neural projection baseline as the number of training costs changes. Additional experiments and details are reported in Section B.

### 4.1 Experimental protocol

We compare our calibrated exact-compression method, denoted OURSESTC, with two projection-learning baselines. The first is DATADRIVENPROJ, a PCA-based data-driven projection method in the spirit of Sakaue and Oki (2024): it learns a shared  $K$ -dimensional projection from training LP instances and then solves the projected LP at test time. The second is FCNN-C, a cost-only neural projection baseline following the neural projection paradigm of Iwata and Sakaue (2025): it maps the observed cost vector to an instance-specific projection and solves the resulting reduced LP.

For OURSESTC, we construct an estimated prior of the form  $\widehat{\mathcal{C}} = \{c : s_{\widehat{\theta}}(c) \leq S_{(k)}\}$ , where  $s_{\widehat{\theta}}$  is the ridge Mahalanobis score from Section A.3.1 and  $S_{(k)}$  is the calibration order statistic associated with the target outside-mass level  $\rho$ . The radius is therefore calibrated from empirical scores. After forming  $\widehat{\mathcal{C}}$ , we run Algorithm 1 on the retained training costs to obtain an affine exact-compression matrix of learned dimension  $d(\rho)$ . The benchmark suite contains the synthetic repeated-LP families and selected Netlib instances used throughout the paper<sup>2</sup>. Accuracy is measured by the average test objective ratio, i.e., the objective value returned by a method divided by the full-LP objective value on the same test instance. The plotted comparisons use twelve retained test seeds. Shaded regions denote standard errors over random seeds.

**Experiment 1: dimension growth under a calibrated estimated prior.** Figure 2 reports the dimension learned by OURSESTC as more historical costs are processed. This experiment uses the calibrated estimated prior with  $\rho = 0.1$ . The quantity plotted is the dimension for the compressed LP. The figure shows that the learned rank stabilizes quickly on several instances, especially MinCostFlow and the RandomLP families, while Packing and GROW7 require larger subspaces. This behavior is exactly what the estimated-prior construction is meant to reveal: the learned dimension is not the ambient cost dimension, but the intrinsic dimension of the optimizer variation inside the calibrated high-mass region. Thus, a small number of informative samples can often identify the relevant affine slice, whereas difficult instances simply manifest themselves as the training proceeds.

**Experiment 2: compression–coverage tradeoff through  $\rho$ .** Figure 3 varies the target outside-mass level  $\rho$ . For each  $\rho$ , OURSESTC constructs a different calibrated set  $\widehat{\mathcal{C}}_{\rho}$ , learns its decision-relevant dimension  $d(\rho)$ , and solves the corresponding affine reduced LP. The projection baselines are then given the same dimensional budget  $K = d(\rho)$ , so the comparison isolates whether the learned dimensions are being used in a decision-sufficient way.

<sup>2</sup>Details of the LP instances and cost distributions are deferred to Appendix B.

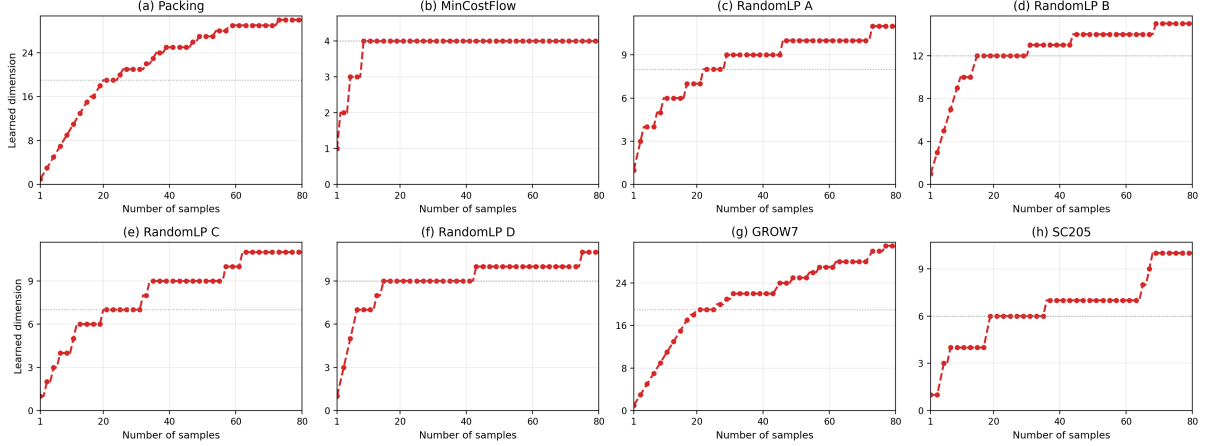


Figure 2: Dimension growth of OURSESTC.

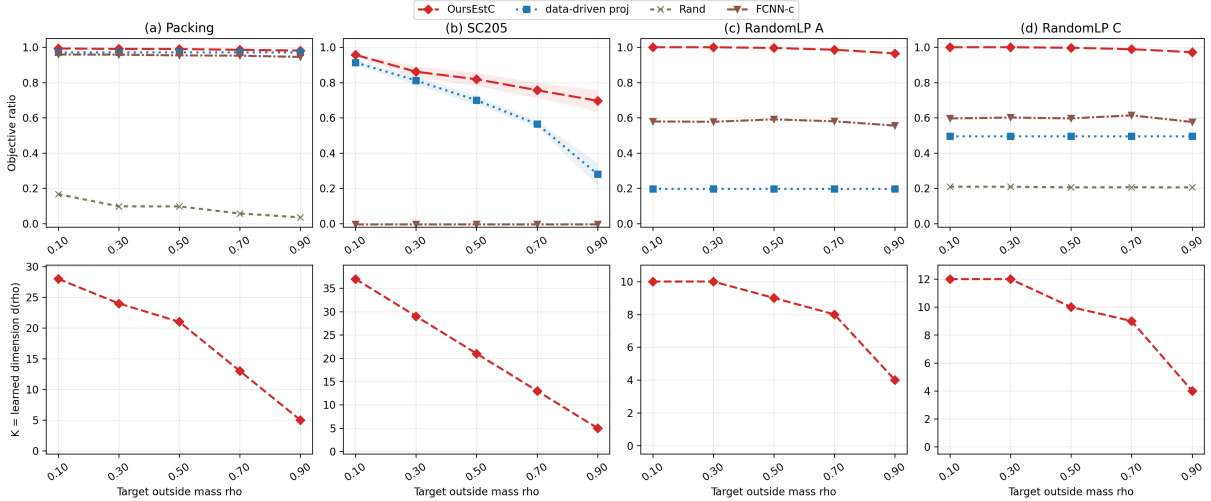


Figure 3: Comparison across target outside-mass levels. Rand corresponds to random projections.

This experiment illustrates the main message of Section 3.3. Increasing  $\rho$  intentionally discards more low-probability cost mass, which can lower  $d(\rho)$  and hence produce a smaller reduced LP. The empirical curves show that this compression can be obtained with little loss on many test instances, while the projection baselines often fail to match the exact method even at the same dimension. In other words, the estimated prior does not merely choose a smaller  $K$ ; it directs the learner toward the optimizer-changing directions inside the high-mass region.

**Experiment 3: comparison against neural projections.** Figure 4 compares the calibrated exact method with the plain-random FCNN-C baseline as the number of training costs varies. For FCNN-C, each dashed curve reports the objective ratio using the displayed number of training samples and one of the reduced dimensions  $K \in \{10, 20, 30, 50\}$ . OURSESTC is shown as a calibrated exact-compression reference, using the working prior and cumulative direction discovery described above. These results indicate that our algorithm works substantially better than the compared baseline.

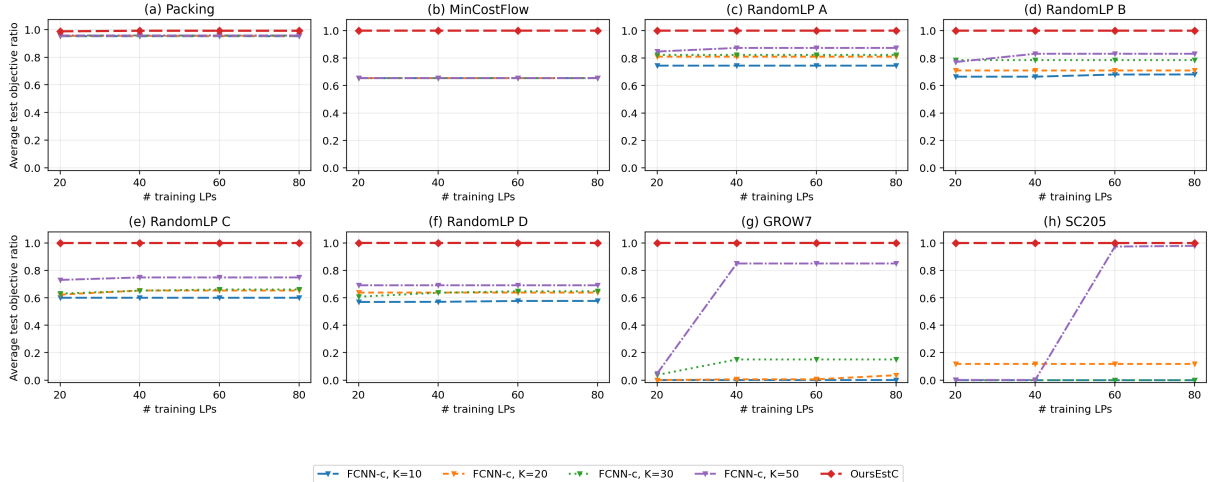


Figure 4: Comparison against the FCNN-c baseline.

## 5 Conclusion and Limitations

We characterized exact compression of repeatedly solved linear programs through the geometry of the decision-relevant subspace  $\text{dir}(\mathcal{X}^*(\mathcal{C}))$ : any affine slice anchored at a reachable optimizer and whose direction subspace contains  $\text{dir}(\mathcal{X}^*(\mathcal{C}))$  yields an exact reformulation, and a basis of  $\text{dir}(\mathcal{X}^*(\mathcal{C}))$  gives the minimal  $d^*$ -variable one. Our sample-based learner grows this basis only on informative instances and comes with a fast  $\tilde{O}(d^*/n)$  out-of-sample certificate, and empirically matches the full-LP objective with a relatively low number of samples.

Two limitations point to natural future directions. First, our experiments provide strong evidence that our approach is stronger than the state of the art on synthetic and Netlib instances, but a broader study on real-world repeated-LP settings is needed to fully characterize the practical speedups. Second, the theory is currently restricted to linear programs; extending the decision-relevant subspace framework to mixed-integer and convex quadratic programs is a promising direction.

## References

- Alessandro Alessio and Alberto Bemporad. A survey on explicit model predictive control. In *Nonlinear Model Predictive Control: Towards New Challenging Applications*, volume 384 of *Lecture Notes in Control and Information Sciences*, pages 345–369. Springer, Berlin, 2009.
- Brandon Amos. Tutorial on amortized optimization. *Foundations and Trends in Machine Learning*, 16(5):592–732, 2023.
- Maria-Florina Balcan. Data-driven algorithm design. In Tim Roughgarden, editor, *Beyond the Worst-Case Analysis of Algorithms*, pages 626–645. Cambridge University Press, 2021.
- Maria-Florina Balcan, Vaishnavh Nagarajan, Ellen Vitercik, and Colin White. Learning-theoretic foundations of algorithm configuration for combinatorial partitioning problems. In *Proceedings of the 30th Conference on Learning Theory*, volume 65 of *Proceedings of Machine Learning Research*, pages 213–274. PMLR, 2017.

- Maria-Florina Balcan, Dan DeBlasio, Travis Dick, Carl Kingsford, Tuomas Sandholm, and Ellen Vitercik. How much data is sufficient to learn high-performing algorithms? Generalization guarantees for data-driven algorithm design. *Journal of the ACM*, 71(5):32:1–32:58, 2024.
- Alberto Bemporad, Manfred Morari, Vivek Dua, and Efstratios N. Pistikopoulos. The explicit linear quadratic regulator for constrained systems. *Automatica*, 38(1):3–20, 2002.
- Omar Bennouna, Amine Bennouna, Saurabh Amin, and Asuman E. Ozdaglar. What data enables optimal decisions? an exact characterization for linear optimization. In *Advances in Neural Information Processing Systems*, volume 38, 2025. NeurIPS 2025.
- Omar Bennouna, Amine Bennouna, Saurabh Amin, and Asuman Ozdaglar. Data informativeness in linear optimization under uncertainty. *arXiv preprint arXiv:2602.15365*, 2026. URL <https://arxiv.org/abs/2602.15365>.
- Dimitris Bertsimas and Bartolomeo Stellato. The voice of optimization. *Machine Learning*, 110(2):249–277, 2021.
- Francesco Borrelli, Alberto Bemporad, and Manfred Morari. *Predictive Control for Linear and Hybrid Systems*. Cambridge University Press, Cambridge, 2017.
- Olivier Bousquet, Steve Hanneke, Shay Moran, and Nikita Zhivotovskiy. Proper learning, Helly number, and an optimal SVM bound. In *Proceedings of the 33rd Conference on Learning Theory*, volume 125 of *Proceedings of Machine Learning Research*, pages 582–609. PMLR, 2020.
- Marco C. Campi and Simone Garatti. Compression, generalization and learning. *Journal of Machine Learning Research*, 24(339):1–74, 2023.
- Tianlong Chen, Xiaohan Chen, Wuyang Chen, Howard Heaton, Jialin Liu, Zhangyang Wang, and Wotao Yin. Learning to optimize: A primer and a benchmark. *Journal of Machine Learning Research*, 23(189):1–59, 2022.
- Claudia d’Ambrosio, Leo Liberti, Pierre-Louis Poirion, and Ky Vu. Random projections for quadratic programs. *Mathematical Programming*, 183(1–2):619–647, 2020.
- Othman El Balghiti, Adam N. Elmachtoub, Paul Grigas, and Ambuj Tewari. Generalization bounds in the predict-then-optimize framework. *Mathematics of Operations Research*, 48(4):2043–2065, 2023.
- Anthony V. Fiacco. *Introduction to Sensitivity and Stability Analysis in Nonlinear Programming*, volume 165 of *Mathematics in Science and Engineering*. Academic Press, New York, 1983.
- Sally Floyd and Manfred K. Warmuth. Sample compression, learnability, and the vapnik–chervonenkis dimension. *Machine Learning*, 21(3):269–304, 1995.
- Thore Graepel, Ralf Herbrich, and John Shawe-Taylor. PAC-bayesian compression bounds on the prediction error of learning algorithms for classification. *Machine Learning*, 59(1–2):55–76, 2005.
- Rishi Gupta and Tim Roughgarden. A PAC approach to application-specific algorithm selection. *SIAM Journal on Computing*, 46(3):992–1017, 2017.
- Rishi Gupta and Tim Roughgarden. Data-driven algorithm design. *Communications of the ACM*, 63(6):87–94, 2020.

- Steve Hanneke and Aryeh Kontorovich. A sharp lower bound for agnostic learning with sample compression schemes. In *Proceedings of the 30th International Conference on Algorithmic Learning Theory*, volume 98 of *Proceedings of Machine Learning Research*, pages 489–505. PMLR, 2019.
- Steve Hanneke and Aryeh Kontorovich. Stable sample compression schemes: New applications and an optimal SVM margin bound. In Vitaly Feldman, Katrina Ligett, and Sivan Sabato, editors, *Proceedings of the 32nd International Conference on Algorithmic Learning Theory*, volume 132 of *Proceedings of Machine Learning Research*, pages 697–721. PMLR, 2021.
- Tomoharu Iwata and Shinsaku Sakaue. Learning to generate projections for reducing dimensionality of heterogeneous linear programming problems. In *Proceedings of the 42nd International Conference on Machine Learning*, 2025.
- Olivier Ledoit and Michael Wolf. A well-conditioned estimator for large-dimensional covariance matrices. *Journal of Multivariate Analysis*, 88(2):365–411, 2004.
- Jing Lei, Max G'Sell, Alessandro Rinaldo, Ryan J. Tibshirani, and Larry Wasserman. Distribution-free predictive inference for regression. *Journal of the American Statistical Association*, 113(523):1094–1111, 2018.
- Nick Littlestone and Manfred K. Warmuth. Relating data compression and learnability. Technical report, University of California, Santa Cruz, 1986.
- Prasanta Chandra Mahalanobis. On the generalized distance in statistics. *Proceedings of the National Institute of Sciences of India*, 2(1):49–55, 1936.
- Sidhant Misra, Line Roald, and Yeesian Ng. Learning for constrained optimization: Identifying optimal active constraint sets. *INFORMS Journal on Computing*, 34(1):463–480, 2022.
- Shay Moran and Amir Yehudayoff. Sample compression schemes for VC classes. *Journal of the ACM*, 63(3):21:1–21:10, 2016.
- Anh Tuan Nguyen and Viet Anh Nguyen. Provably data-driven projection method for quadratic programming. *Proceedings of the AAAI Conference on Artificial Intelligence*, 40(29):24541–24548, 2026.
- Pierre-Louis Poirion, Bruno F. Lourenço, and Akiko Takeda. Random projections of linear and semidefinite problems with linear inequalities. *Linear Algebra and its Applications*, 664:24–60, 2023.
- Shinsaku Sakaue and Taihei Oki. Generalization bound and learning methods for data-driven projections in linear programming. In *Advances in Neural Information Processing Systems*, 2024.
- Rajiv Sambharya, Georgina Hall, Brandon Amos, and Bartolomeo Stellato. Learning to warm-start fixed-point optimization algorithms. *Journal of Machine Learning Research*, 25(166):1–46, 2024.
- Leslie G. Valiant. A theory of the learnable. *Communications of the ACM*, 27(11):1134–1142, 1984.
- Vladimir Vovk, Alex Gammerman, and Glenn Shafer. *Algorithmic Learning in a Random World*. Springer, 2005.
- Ky Vu, Pierre-Louis Poirion, and Leo Liberti. Random projections for linear programming. *Mathematics of Operations Research*, 43(4):1051–1071, 2018.

Samuel S. Wilks. Determination of sample sizes for setting tolerance limits. *The Annals of Mathematical Statistics*, 12(1):91–96, 1941.

Yuhan Ye, Saurabh Amin, and Asuman E. Ozdaglar. Learning decision-sufficient representations for linear optimization. *arXiv preprint arXiv:2603.18551*, 2026. URL <https://arxiv.org/abs/2603.18551>. Accepted to COLT 2026.

## A Deferred proofs

### A.1 Delayed proofs in Subsection 3.1

*Proof of Theorem 2.* Suppose first that  $V$  is exact-sketching on  $\mathcal{C}$ . Then every reachable optimizer belongs to  $V$ : if  $v \in \mathcal{X}^*(\mathcal{C})$ , then for some  $c \in \mathcal{C}$  we have  $v \in \arg \min_{x \in \mathcal{X}} c^\top x$ , and exactness gives  $v \in \arg \min_{x \in \mathcal{X} \cap V} c^\top x \subseteq V$ . Hence  $V \cap \mathcal{X}^*(\mathcal{C}) \neq \emptyset$ . Moreover, for any  $v, v' \in \mathcal{X}^*(\mathcal{C})$ , both points lie in  $V$ , so  $v - v' \in \text{dir}(V)$ . Taking spans over all such pairs yields  $\text{dir}(\mathcal{X}^*(\mathcal{C})) \subseteq \text{dir}(V)$ .

Conversely, assume  $\text{dir}(\mathcal{X}^*(\mathcal{C})) \subseteq \text{dir}(V)$  and choose  $x_0 \in V \cap \mathcal{X}^*(\mathcal{C})$ . For every  $v \in \mathcal{X}^*(\mathcal{C})$ , we have  $v - x_0 \in \text{dir}(\mathcal{X}^*(\mathcal{C})) \subseteq \text{dir}(V)$ , so  $v \in V$ . Thus  $V$  contains all reachable optimizers. Fix  $c \in \mathcal{C}$ . The optimal face  $\arg \min_{x \in \mathcal{X}} c^\top x$  is the convex hull of its extreme points, and these extreme points belong to  $\mathcal{X}^*(\mathcal{C})$ . Therefore the whole optimal face is contained in  $V$ . Hence, the restricted and original LPs have the same optimizer set, and  $V$  is exact-sketching on  $\mathcal{C}$ .  $\square$

*Justification of (4) and (Exact( $U, x_0, c$ )).* Let  $V := x_0 + \text{range}(U)$ . Under the assumptions stated before (Exact( $U, x_0, c$ )), Theorem 2 gives

$$\arg \min_{x \in \mathcal{X} \cap V} c^\top x = \mathcal{X}^*(c), \quad c \in \mathcal{C}.$$

The map  $T_{U, x_0}$  is an affine bijection from  $\mathcal{Z}_{U, x_0}$  onto  $\mathcal{X} \cap V$ , and  $c^\top T_{U, x_0}(z) = c^\top x_0 + (U^\top c)^\top z$ . Therefore

$$T_{U, x_0}(F_{U, x_0}(c)) = \arg \min_{x \in \mathcal{X} \cap V} c^\top x = \mathcal{X}^*(c),$$

which is (Exact( $U, x_0, c$ )). The same parametrization gives

$$\min_{x \in \mathcal{X}} c^\top x = \min_{x \in \mathcal{X} \cap V} c^\top x = c^\top x_0 + \min_{z \in \mathcal{Z}_{U, x_0}} (U^\top c)^\top z,$$

which is (4).  $\square$

*Proof of Corollary 3.* Let  $F_Z := F_{U, x_0}(c)$  and  $F_X := \mathcal{X}^*(c)$ . Exactness gives  $T_{U, x_0}(F_Z) = F_X$ . Since  $T_{U, x_0}$  is an affine bijection from  $\mathcal{Z}_{U, x_0}$  onto  $\mathcal{X} \cap V_{U, x_0}$ , it is also an affine bijection from the face  $F_Z$  onto the face  $F_X$ . Hence it maps extreme points of  $F_Z$  exactly to extreme points of  $F_X$ :

$$T_{U, x_0}(F_Z^\angle) = F_X^\angle.$$

Because  $F_Z$  is a face of  $\mathcal{Z}_{U, x_0}$ ,  $F_Z^\angle = F_Z \cap \mathcal{Z}_{U, x_0}^\angle$ . Because  $F_X$  is a face of  $\mathcal{X}$ ,  $F_X^\angle = F_X \cap \mathcal{X}^\angle$ . Substituting these identities yields

$$T_{U, x_0}(F_{U, x_0}(c) \cap \mathcal{Z}_{U, x_0}^\angle) = \mathcal{X}^*(c) \cap \mathcal{X}^\angle.$$

$\square$

*Verification of Example 4.* For every  $c \in \mathcal{C}_\rho$ ,  $c_1 < 0$ , so every minimizer over  $[-1, 1]^2$  has  $x_1 = 1$ . If  $c_2 > 0$  the unique optimizer is  $(1, -1)$ , if  $c_2 < 0$  it is  $(1, 1)$ , and if  $c_2 = 0$  the whole right edge is optimal. Since  $0 \in (-1, 1)$ , the reachable optimizer set is therefore

$$\mathcal{X}^*(\mathcal{C}_\rho) = \{1\} \times [-1, 1], \quad \text{dir}(\mathcal{X}^*(\mathcal{C}_\rho)) = \text{span}\{(0, 1)\}.$$

Thus the affine slice  $(1, 0) + \text{span}\{(0, 1)\}$  gives the exact one-variable reduction  $x = (1, z)$ ,  $z \in [-1, 1]$ .

Now fix any one-dimensional homogeneous subspace  $L$ . Write  $[-1, 1]^2 \cap L = \{\lambda z : \lambda \in [-1, 1]\}$  for some  $z \in [-1, 1]^2$ . Let a uniform cost be  $c = (-A, B)$ , where  $A \sim \text{Unif}(1, 1 + \rho)$  and  $B \sim \text{Unif}(-1, 1)$  are independent. The full value is

$$\text{val}(c) = -A - |B|,$$

whereas the value restricted to  $L$  is

$$\text{val}_L(c) = \min_{\lambda \in [-1, 1]} \lambda(-Az_1 + Bz_2) = -| -Az_1 + Bz_2|.$$

Condition on  $A$  and  $T := |B|$ . Averaging over the two signs of  $B$  and using  $|p + q| + |p - q| = 2 \max\{|p|, |q|\}$ , we get

$$\mathbb{E}[| -Az_1 + Bz_2| \mid A, T] = \max\{A|z_1|, T|z_2|\} \leq A,$$

since  $T \leq 1 \leq A$  and  $|z_1|, |z_2| \leq 1$ . Therefore

$$\mathbb{E}[\text{val}_L(c) - \text{val}(c) \mid A, T] = A + T - \mathbb{E}[| -Az_1 + Bz_2| \mid A, T] \geq T.$$

Finally,  $T = |B| \sim \text{Unif}(0, 1)$ , so  $\mathbb{E}[T] = 1/2$ . Hence, every one-dimensional homogeneous slice has an expected objective gap of at least  $1/2$ .  $\square$

## A.2 Delayed proofs in Subsection 3.2

We first provide a geometric characterization of  $\text{Exact}(U, x_0, c)$ .

**Lemma 8** (Characterization of  $\text{Exact}(U, x_0, c)$ ). *Fix  $x_0 \in \mathcal{X}$  and a full-column-rank matrix  $U$ , and set*

$$V_{U, x_0} := x_0 + \text{range}(U).$$

For any  $c \in \mathbb{R}^d$ ,

$$\text{Exact}(U, x_0, c) \iff \mathcal{X}^*(c) \subseteq V_{U, x_0}.$$

Consequently, if  $U^+$  is obtained from  $U$  by appending columns and  $\text{Exact}(U, x_0, c)$  holds, then  $\text{Exact}(U^+, x_0, c)$  holds.

*Proof.* The map  $T_{U, x_0}$  is an affine bijection from  $\mathcal{Z}_{U, x_0}$  onto  $\mathcal{X} \cap V_{U, x_0}$ . Hence

$$T_{U, x_0}(F_{U, x_0}(c)) = \arg \min_{x \in \mathcal{X} \cap V_{U, x_0}} c^\top x.$$

If  $\text{Exact}(U, x_0, c)$  holds, then the right-hand side is  $\mathcal{X}^*(c)$ , so  $\mathcal{X}^*(c) \subseteq V_{U, x_0}$ .

Conversely, suppose  $\mathcal{X}^*(c) \subseteq V_{U, x_0}$ . Since  $\mathcal{X} \cap V_{U, x_0} \subseteq \mathcal{X}$ , the restricted LP cannot have value smaller than the original LP. On the other hand, the original optimal face  $\mathcal{X}^*(c)$  is feasible for the restricted LP by assumption. Thus the two optimal values are equal, and the restricted optimizer set is

$$\arg \min_{x \in \mathcal{X} \cap V_{U, x_0}} c^\top x = \mathcal{X}^*(c) \cap V_{U, x_0} = \mathcal{X}^*(c).$$

This is exactly  $\text{Exact}(U, x_0, c)$ .

Finally, appending columns enlarges  $V_{U, x_0}$ . Therefore containment of the optimal face is preserved, and the monotonicity statement follows from the equivalence just proved.  $\square$

To proceed, we show that the containment test-and-append process in Lines 6–7 of Algorithm 1 can be implemented by solving LPs.

**Lemma 9** (Containment test via LPs). *Fix  $c \in \mathbb{R}^d$ , an anchor  $x_0 \in \mathcal{X}$ , and a matrix  $U$ . Let  $S := \text{range}(U)$ , let*

$$v(c) := \min_{y \in \mathcal{X}} c^\top y, \quad G(c) := \mathcal{X}^*(c) = \{x \in \mathcal{X} : c^\top x = v(c)\},$$

and let  $a_1, \dots, a_{d-r}$  be any basis of  $S^\perp$ , where  $r := \text{rank}(U)$ . Then

$$G(c) \subseteq x_0 + S$$

if and only if, for every  $j = 1, \dots, d-r$ ,

$$\max_{x \in G(c)} a_j^\top (x - x_0) = 0 \quad \text{and} \quad \min_{x \in G(c)} a_j^\top (x - x_0) = 0.$$

Moreover, if the containment fails, then one of these auxiliary LPs returns an extreme optimizer  $x \in G(c) \cap \mathcal{X}^\angle$  satisfying  $x - x_0 \notin S$ .

*Proof.* For any  $x \in \mathbb{R}^d$ , we have  $x \in x_0 + S$  if and only if  $x - x_0 \in S$ , which is equivalent to

$$a_j^\top (x - x_0) = 0 \quad \text{for all } j = 1, \dots, d-r.$$

Therefore  $G(c) \subseteq x_0 + S$  holds if and only if each of the linear functionals  $a_j^\top (x - x_0)$  is identically zero on  $G(c)$ . This is equivalent to requiring both its maximum and its minimum over  $G(c)$  to be zero.

If the containment fails, then for some  $j$  there exists  $\bar{x} \in G(c)$  with  $a_j^\top (\bar{x} - x_0) \neq 0$ . Hence either

$$\max_{x \in G(c)} a_j^\top (x - x_0) > 0 \quad \text{or} \quad \min_{x \in G(c)} a_j^\top (x - x_0) < 0.$$

Choose an extreme optimal solution of the corresponding auxiliary LP over  $G(c)$ . Since  $G(c)$  is a face of the polytope  $\mathcal{X}$ , every extreme point of  $G(c)$  is an extreme point of  $\mathcal{X}$ . The chosen point therefore belongs to  $G(c) \cap \mathcal{X}^\angle$  and has nonzero projection along some  $a_j \in S^\perp$ , so  $x - x_0 \notin S$ .  $\square$

The next three lemmas formalize the key structural properties of our algorithm. Together, they show that Algorithm 1 induces a *stable, realizable* sample compression scheme (Hanneke and Kontorovich, 2021, Definitions 7–8) with compression size at most  $d^*$ . This is the key mechanism we use to obtain a distribution-free fast-rate certificate (5).

**Lemma 10** (Compression size and termination). *Fix an anchor  $x_0 \in \mathcal{X}^*(\mathcal{C})$  and run Algorithm 1 with deterministic tie-breaking. Then the algorithm makes at most  $d^*$  total appends. Moreover, for its output  $(U_n, T_n)$ ,*

$$\text{range}(U_n) \subseteq \text{dir}(\mathcal{X}^*(\mathcal{C})), \quad |T_n| \leq \text{rank}(U_n) \leq d^*.$$

*Proof.* Every appended column has the form  $x - x_0$ , where  $x \in \mathcal{X}^*(c_i) \cap \mathcal{X}^\angle$  for some training sample  $c_i \in \mathcal{C}$ . Since  $x \in \mathcal{X}^*(\mathcal{C})$  and  $x_0 \in \mathcal{X}^*(\mathcal{C})$ , we have

$$x - x_0 \in \text{dir}(\mathcal{X}^*(\mathcal{C})).$$

Thus every appended direction lies in  $\text{dir}(\mathcal{X}^*(\mathcal{C}))$ .

The update rule appends such a vector only when  $x - x_0 \notin \text{range}(U_i)$ . Hence each append increases the rank of the current matrix by exactly one. Starting from the empty matrix, after  $k$  appends the current rank is  $k$ , and its range is a  $k$ -dimensional subspace of  $\text{dir}(\mathcal{X}^*(\mathcal{C}))$ . Since  $\dim(\text{dir}(\mathcal{X}^*(\mathcal{C}))) = d^*$ , there can be at most  $d^*$  appends.

This also proves termination: if the while-loop were still active after the current range had dimension  $d^*$ , then the algorithm would find  $x \in \mathcal{X}^*(c_i) \cap \mathcal{X}^{\setminus}$  with  $x - x_0 \notin \text{range}(U_i)$ . But all such differences belong to  $\text{dir}(\mathcal{X}^*(\mathcal{C}))$ , and the current range is already a  $d^*$ -dimensional subspace of  $\text{dir}(\mathcal{X}^*(\mathcal{C}))$ , hence equals  $\text{dir}(\mathcal{X}^*(\mathcal{C}))$ , a contradiction.

Finally, every hard sample triggers at least one append, while each append increases the rank by one. Therefore

$$|T_n| \leq \text{rank}(U_n) \leq d^*,$$

and the range inclusion follows from the first paragraph.  $\square$

**Lemma 11** (Realizability). *Under the assumptions of Lemma 10, the output  $U_n$  of Algorithm 1 satisfies*

$$\text{Exact}(U_n, x_0, c_i) \quad \text{for every } i = 1, \dots, n.$$

*Equivalently, the empirical failure loss  $1\{\neg \text{Exact}(U_n, x_0, c_i)\}$  is zero on the training sample.*

*Proof.* Fix a training index  $i$ . When the while-loop for  $c_i$  terminates, it has certified

$$\mathcal{X}^*(c_i) \subseteq x_0 + \text{range}(U_i).$$

By Lemma 8, this is equivalent to  $\text{Exact}(U_i, x_0, c_i)$ .

For later samples  $t > i$ , Algorithm 1 only appends columns to the matrix. Therefore

$$\text{range}(U_i) \subseteq \text{range}(U_t) \quad \text{for all } t \geq i.$$

The monotonicity statement in Lemma 8 then implies  $\text{Exact}(U_n, x_0, c_i)$ .  $\square$

**Lemma 12** (Stability). *Let  $S = (c_1, \dots, c_n)$  be the training sequence and let  $(U_n, T_n)$  be the output of Algorithm 1. Write*

$$T_n = \{i_1 < \dots < i_k\}, \quad S_T := (c_{i_1}, \dots, c_{i_k})$$

*for the ordered hard subsequence. If Algorithm 1 is rerun on  $S_T$  using the same fixed anchor  $x_0$  and the same deterministic containment-and-update rule, then it returns the same matrix  $U_n$ . More generally, deleting any subset of the non-hard samples from  $S$  leaves the reconstructed output unchanged.*

*Proof.* Let  $U^{(j)}$  denote the matrix in the original run immediately after processing the hard sample  $c_{i_j}$ , and set  $U^{(0)}$  to be the empty matrix. We prove by induction on  $j$  that rerunning the algorithm on the first  $j$  hard samples  $(c_{i_1}, \dots, c_{i_j})$  produces exactly  $U^{(j)}$ .

For  $j = 0$  this is immediate. Before the first hard index  $i_1$ , every sample in the original run is non-hard and hence leaves the empty matrix unchanged. Thus  $c_{i_1}$  enters the original run with matrix  $U^{(0)}$ . The reconstructed run also feeds  $c_{i_1}$  into the same matrix  $U^{(0)}$ . Since the containment tests, outside-vertex choices, and all tie-breaking rules are fixed deterministically, the full while-loop for  $c_{i_1}$  appends the same sequence of directions in both runs. Hence the reconstructed matrix after  $c_{i_1}$  is  $U^{(1)}$ .

Now assume the claim holds through hard sample  $c_{i_j}$ . In the original run, all samples between  $i_j$  and  $i_{j+1}$  are non-hard, so they leave the matrix  $U^{(j)}$  unchanged. Hence  $c_{i_{j+1}}$  enters the original run

with matrix  $U^{(j)}$ . By the induction hypothesis, the reconstructed run also presents  $c_{i_{j+1}}$  to the same matrix  $U^{(j)}$ . Determinism again forces the same sequence of appends, so the reconstructed matrix after  $c_{i_{j+1}}$  is  $U^{(j+1)}$ .

Taking  $j = k$  shows that rerunning the algorithm only on the ordered hard subsequence  $S_T$  reproduces  $U_n$ . If some non-hard samples are retained while others are deleted, the same induction applies: retained non-hard samples enter with the same matrix as in the original run and perform no append. Thus deleting any subset of non-hard samples does not change the final reconstructed matrix.  $\square$

We now provide the full proof of Theorem 5.

*Proof of Theorem 5.* The structural claims

$$\text{range}(U_n) \subseteq \text{dir}(\mathcal{X}^*(\mathcal{C})), \quad |T_n| \leq \text{rank}(U_n) \leq d^*$$

are exactly Lemma 10. The zero-training-failure claim is Lemma 11. It remains to prove the out-of-sample certificate (5).

**Sample-compression background.** Sample compression is a classical way to prove distribution-free generalization: rather than controlling the complexity of an entire hypothesis class, one shows that the learned predictor can be reconstructed from a small subset of the training sample. This idea goes back to the PAC-learning and compression literature (Valiant, 1984; Littlestone and Warmuth, 1986; Floyd and Warmuth, 1995); see also Graepel et al. (2005); Moran and Yehudayoff (2016) for later developments. The particular form needed here is the *stable, realizable* version of sample compression. Stable compression schemes and their fast-rate consequences are developed in Bousquet et al. (2020) and Hanneke and Kontorovich (2021); related compression-based certificates in optimization and scenario analysis are discussed by Campi and Garatti (2023).

We recall the specific form used below. A sample compression scheme for binary prediction consists of a compression map  $\kappa$ , which selects an ordered subsequence of the training sample, and a reconstruction map  $\rho$ , which maps the compressed subsequence to a prediction rule. The scheme is *stable* if deleting any uncompressed training examples does not change the reconstructed rule. In the *realizable stable* case, where the reconstructed rule has zero empirical error, Hanneke and Kontorovich (2021, Definitions 7–8 and Corollary 11) imply that, with probability at least  $1 - \delta$  over an i.i.d. sample  $S$  of size  $n$ ,

$$R(\rho(\kappa(S))) \leq \frac{4}{n} \left( 6|\kappa(S)| + \log \frac{e}{\delta} \right),$$

where  $R(\cdot)$  is the true 0–1 risk and  $|\kappa(S)|$  is the realized compression size. This fast  $1/n$  rate is specific to the realizable stable regime; in agnostic compression settings, such fast rates are not available in general (Hanneke and Kontorovich, 2019).

**The induced binary learning problem.** For a matrix  $U$ , define the binary failure rule

$$h_U(c) := 1\{\neg \text{Exact}(U, x_0, c)\}.$$

Equivalently, we may view the data as a supervised binary problem with examples  $(c, Y)$ , where  $c \sim P_c$  and  $Y = 0$  almost surely. Under this convention, the risk of  $h_U$  is exactly the exact-compression failure probability:

$$R(h_U) = \mathbb{P}_{c \sim P_c}[h_U(c) = 1] = \mathbb{P}_{c \sim P_c}[\neg \text{Exact}(U, x_0, c)].$$

Let  $S = (c_1, \dots, c_n)$  and let  $(U_n, T_n)$  be the output of Algorithm 1. Define the compression map  $\kappa$  by

$$\kappa(S) := (c_i)_{i \in T_n},$$

where the subsequence is stored in its original order. Since all labels are identically zero, we suppress them in the notation; equivalently,  $\kappa$  stores the labeled examples  $(c_i, 0)_{i \in T_n}$ . Define the reconstruction map  $\rho$  by rerunning Algorithm 1 on any supplied subsequence  $S'$  using the same fixed anchor  $x_0$  and the same deterministic rule, and returning the classifier  $h_{U(S')}$  induced by the resulting matrix  $U(S')$ .

By Lemma 12, rerunning the algorithm on the compressed hard subsequence  $\kappa(S)$  returns the same matrix  $U_n$ . Therefore

$$\rho(\kappa(S)) = h_{U_n}.$$

The same lemma also gives the stability property required by Hanneke and Kontorovich (2021): deleting any subset of the uncompressed samples does not change the reconstructed classifier. By Lemma 11,

$$h_{U_n}(c_i) = 0 \quad \text{for every } i = 1, \dots, n,$$

so the reconstructed classifier has zero empirical error.

Applying Hanneke and Kontorovich (2021, Corollary 11) to this stable realizable compression scheme yields, with probability at least  $1 - \delta$ ,

$$\begin{aligned} \mathbb{P}_{c \sim P_c}[\neg \text{Exact}(U_n, x_0, c)] &= R(h_{U_n}) \\ &= R(\rho(\kappa(S))) \\ &\leq \frac{4}{n} \left( 6|\kappa(S)| + \log \frac{e}{\delta} \right) \\ &= \frac{4}{n} \left( 6|T_n| + \log \frac{e}{\delta} \right). \end{aligned}$$

Taking complements gives

$$\mathbb{P}_{c \sim P_c}[\text{Exact}(U_n, x_0, c)] \geq 1 - \frac{4}{n} \left( 6|T_n| + \log \frac{e}{\delta} \right).$$

The final inequality in the theorem follows from  $|T_n| \leq d^*$  in Lemma 10.

**Anchor generated from data.** The theorem assumes that  $x_0$  is fixed independently of the  $n$  training costs. If instead  $x_0$  is generated from one of the training samples, then the same compression argument remains valid after adding the anchor-generating sample to the compressed subsequence and letting the reconstruction map first recompute  $x_0$  by the same deterministic rule. The bound is then unchanged except that  $|T_n|$  is replaced by  $|T_n| + 1$ . Equivalently, one may draw an independent anchor sample first and apply the theorem to the remaining representation-learning samples.

**LP implementation and tractability.** It remains to justify the claimed LP-based implementation. By Lemma 9, each containment test

$$\mathcal{X}^*(c_i) \subseteq x_0 + \text{range}(U_i)$$

can be implemented by first solving the LP defining  $v(c_i)$  and then solving, for a basis  $a_1, \dots, a_{d-r}$  of  $\text{range}(U_i)^\perp$ , the auxiliary LPs

$$\max_{x \in \mathcal{X}: c_i^\top x = v(c_i)} a_j^\top (x - x_0), \quad \min_{x \in \mathcal{X}: c_i^\top x = v(c_i)} a_j^\top (x - x_0).$$

If all these optima are zero, containment is certified. If not, an extreme optimal solution of a violated auxiliary LP is a valid vertex  $x \in \mathcal{X}^*(c_i) \cap \mathcal{X}^{\angle}$  with  $x - x_0 \notin \text{range}(U_i)$ , so it is a valid update direction in Algorithm 1.

There is one final containment check for each of the  $n$  samples and one additional check for each append. Since Lemma 10 gives at most  $d^*$  total appends, the number of containment checks is at most  $n + d^*$ . Each check solves only a polynomial number of LPs over  $\mathcal{X}$  or over the optimal face of  $\mathcal{X}$  obtained by adding the equality  $c_i^\top x = v(c_i)$ , and the required orthogonal bases and rank tests are computable by standard linear algebra. Thus, when  $\mathcal{X}$  is given in the H-representation of (2), the cumulative learner is polynomial time in the usual LP oracle model.  $\square$

### A.3 Delayed proofs in Subsection 3.3

#### A.3.1 Construction of calibrated estimated priors

The following construction is distribution-free. It is the one-sided tolerance-region argument of Wilks (1941), written in the language of arbitrary data-fitted scores and closely related to split conformal calibration (Vovk et al., 2005; Lei et al., 2018): Split an independent pilot sample into a fitting sample  $\mathcal{D}_{\text{fit}}$  and a calibration sample  $\mathcal{D}_{\text{cal}} = \{c_1^{\text{cal}}, \dots, c_m^{\text{cal}}\}$ . Fit a measurable score  $s_{\hat{\theta}} : \mathbb{R}^d \rightarrow \mathbb{R}$  using only  $\mathcal{D}_{\text{fit}}$ , and assume every sublevel set  $\{c : s_{\hat{\theta}}(c) \leq t\}$  is convex. Let  $S_j = s_{\hat{\theta}}(c_j^{\text{cal}})$ , write  $S_{(1)} \leq \dots \leq S_{(m)}$  for the order statistics, and set  $S_{(m+1)} := +\infty$ .

Fix  $\rho, \delta_0 \in (0, 1)$ . Define

$$k_{\rho, \delta_0} := \min \{k \in \{1, \dots, m+1\} : \mathbb{P}[\text{Bin}(m, 1-\rho) \geq k] \leq \delta_0\}, \quad \hat{\mathcal{C}}_{\rho, \delta_0} := \{c : s_{\hat{\theta}}(c) \leq S_{(k_{\rho, \delta_0})}\}.$$

Here  $\text{Bin}(m, 1-\rho)$  is the binomial count of calibration scores falling below a population  $(1-\rho)$ -quantile of the fitted score distribution. Thus  $k_{\rho, \delta_0}$  is the upper  $\delta_0$  tail cutoff, roughly  $m(1-\rho) + O\left(\sqrt{m\rho(1-\rho)\log(1/\delta_0)} + \log(1/\delta_0)\right)$ .<sup>3</sup> If the calibration sample is too small for the requested confidence, we set  $k_{\rho, \delta_0} = m+1$  and the calibrated set is all of  $\mathbb{R}^d$ .

**Proposition 13** (Tolerance-calibrated convex estimated prior). *Under the preceding calibration setup,  $\hat{\mathcal{C}}_{\rho, \delta_0}$  is convex and is a  $(\rho, \delta_0)$ -estimated prior.*

A simple score with convex sublevel sets is the ridge Mahalanobis score  $s_{\hat{\theta}}(c) := (c - \hat{\mu})^\top (\hat{\Sigma} + \lambda I)^{-1} (c - \hat{\mu})$ , where  $\lambda > 0$  and  $\hat{\mu}, \hat{\Sigma}$  are fitted on  $\mathcal{D}_{\text{fit}}$ . This is the squared Mahalanobis distance (Mahalanobis, 1936) computed with a ridge covariance estimate; the ridge term makes the inverse well-defined and stabilizes high-dimensional covariance estimation (Ledoit and Wolf, 2004). Its calibrated estimated prior is an ellipsoid.

*Proof of Proposition 13.* Condition on the fitting sample  $\mathcal{D}_{\text{fit}}$ , so the score  $s_{\hat{\theta}}$  is fixed. Let  $S = s_{\hat{\theta}}(c)$  for an independent fresh draw  $c \sim P_c$ , and write  $F(t) := \mathbb{P}[S \leq t]$ . Let

$$q_{1-\rho} := \inf\{t \in \mathbb{R} : F(t) \geq 1-\rho\}$$

be a  $(1-\rho)$ -quantile of the score distribution. By right-continuity of  $F$ ,  $F(q_{1-\rho}) \geq 1-\rho$ , and  $F(q_{1-\rho}^-) := \mathbb{P}[S < q_{1-\rho}] \leq 1-\rho$ .

If  $F(S_{(k)}) < 1-\rho$ , then  $S_{(k)} < q_{1-\rho}$ . Hence at least  $k$  of the calibration scores are strictly smaller than  $q_{1-\rho}$ . The number of such scores has distribution  $\text{Bin}(m, F(q_{1-\rho}^-))$  and is stochastically

<sup>3</sup>A formal derivation of this order estimate is given in Lemma 14.

dominated by  $\text{Bin}(m, 1 - \rho)$ . Therefore, for  $k = k_{\rho, \delta_0}$ ,

$$\begin{aligned} \mathbb{P}_{\text{cal}}[F(S_{(k)}) < 1 - \rho \mid \mathcal{D}_{\text{fit}}] &\leq \mathbb{P}[\text{Bin}(m, F(q_{1-\rho}^-)) \geq k] \\ &\leq \mathbb{P}[\text{Bin}(m, 1 - \rho) \geq k] \leq \delta_0. \end{aligned}$$

Equivalently, with conditional probability at least  $1 - \delta_0$ ,  $P_c(c \in \widehat{\mathcal{C}}_{\rho, \delta_0}) = F(S_{(k)}) \geq 1 - \rho$ . The same conclusion holds after removing the conditioning on  $\mathcal{D}_{\text{fit}}$ . Convexity follows because  $\widehat{\mathcal{C}}_{\rho, \delta_0}$  is a sublevel set of  $s_{\widehat{\theta}}$ ; if  $k = m + 1$ , then  $S_{(m+1)} = +\infty$  and the set is all of  $\mathbb{R}^d$ .  $\square$

**Lemma 14** (Size of the binomial tolerance cutoff). *Let  $X \sim \text{Bin}(m, 1 - \rho)$  and  $L := \log(1/\delta_0)$ . Then*

$$k_{\rho, \delta_0} \leq \min \left\{ m + 1, \left\lfloor m(1 - \rho) + \sqrt{2m\rho(1 - \rho)L} + \frac{2L}{3} \right\rfloor + 1 \right\}.$$

Consequently,  $k_{\rho, \delta_0} = m(1 - \rho) + O\left(\sqrt{m\rho(1 - \rho)\log(1/\delta_0)} + \log(1/\delta_0)\right)$  whenever the cutoff is not forced to be  $m + 1$ .

*Proof.* The Bernstein–Chernoff bound for a binomial random variable gives, for every  $t \geq 0$ ,

$$\mathbb{P}[X - m(1 - \rho) \geq t] \leq \exp\left(-\frac{t^2}{2(m\rho(1 - \rho) + t/3)}\right).$$

With  $t = \sqrt{2m\rho(1 - \rho)L} + 2L/3$ , the exponent is at least  $L$ , hence  $\mathbb{P}[X \geq m(1 - \rho) + t] \leq e^{-L} = \delta_0$ . Therefore any integer strictly larger than  $m(1 - \rho) + t$  is feasible in the definition of  $k_{\rho, \delta_0}$ ; the displayed bound follows after truncating at  $m + 1$ .  $\square$

*Proof of Theorem 7.* By the  $(\rho, \delta_0)$ -estimated-prior property,  $\mathbb{P}_{\text{pilot}}(\mathcal{E}_0) \geq 1 - \delta_0$ . Condition on a pilot realization in  $\mathcal{E}_0$ . Then  $P_c(c \in \widehat{\mathcal{C}}) \geq 1 - \rho > 0$ , so  $P_{\widehat{\mathcal{C}}} = P_c(\cdot \mid c \in \widehat{\mathcal{C}})$  is well-defined and supported on the convex prior  $\widehat{\mathcal{C}}$ . The chosen anchor  $\widehat{x}_0$  belongs to  $\mathcal{X}^*(\widehat{\mathcal{C}})$  by construction.

Applying Theorem 5 to the realized prior  $\widehat{\mathcal{C}}$ , the anchor  $\widehat{x}_0$ , and the distribution  $P_{\widehat{\mathcal{C}}}$  gives, with probability at least  $1 - \delta_1$  over the retained representation-learning sample,

$$\mathbb{P}_{c \sim P_{\widehat{\mathcal{C}}}}[\neg \text{Exact}(U_{n_1}, \widehat{x}_0, c)] \leq \frac{4}{n_1} (6\widehat{d}_* + \log(e/\delta_1)).$$

On this event,

$$\begin{aligned} \mathbb{P}_{c \sim P_c}[\neg \text{Exact}(U_{n_1}, \widehat{x}_0, c)] &\leq P_c(c \notin \widehat{\mathcal{C}}) + P_c(c \in \widehat{\mathcal{C}}) \mathbb{P}_{c \sim P_{\widehat{\mathcal{C}}}}[\neg \text{Exact}(U_{n_1}, \widehat{x}_0, c)] \\ &\leq \rho + \frac{4}{n_1} (6\widehat{d}_* + \log(e/\delta_1)). \end{aligned}$$

Taking complements gives (6). A union bound over  $\mathcal{E}_0$  and the retained-sample event gives joint probability at least  $1 - \delta_0 - \delta_1$ . The final statement follows by applying Proposition 13, which supplies a  $(\rho, \delta_0)$ -estimated prior.  $\square$

## B Additional Experimental Details and Results

This appendix collects the experimental material not shown in the main text. Section B.1 reports the natural-prior benchmark, where the learner is given the intended prior set. Section B.2 reports auxiliary diagnostics for the unknown-prior setting beyond the three figures kept in Section 4.

**LP instances and cost distributions.** All experiments use repeated general-form LPs in inequality form,

$$\min_{x \in \mathbb{R}^d} \{c^\top x : Ax \leq b\},$$

where inequalities originally written in the opposite direction are multiplied by  $-1$ , the feasible region  $\mathcal{X} = \{x : Ax \leq b\} \subseteq \mathbb{R}^d$  is fixed, and only the cost vector  $c \in \mathbb{R}^d$  varies. For synthetic instances,  $d$  is the original decision dimension. Netlib instances are preprocessed similarly to [Sakaue and Oki \(2024\)](#), so that each instance is equivalently transformed into the inequality form displayed above. The reported dimension  $d$  is the dimension of the preprocessed LP.

All costs are generated around a nominal objective  $c_0$  in these same general-form coordinates. Table 1 reports its Euclidean norm and coordinate range, together with the radius values used by the generator. Most natural-prior experiments use the additive factor model

$$c = c_0 + U_c \theta, \quad \theta_j = \sigma_j z_j, \quad z_j \stackrel{\text{i.i.d.}}{\sim} \mathcal{N}(0, 1),$$

where  $c_0 \in \mathbb{R}^d$  is the nominal cost vector and  $U_c \in \mathbb{R}^{d \times r_c}$  is the planted cost-variation subspace. The coordinate standard deviations are

$$\sigma_{ij} = \alpha_i R_i \beta_i^{j-1}, \quad j = 1, \dots, r_c,$$

for instance  $i$ . The exact learner in the known-prior experiment is given the ball  $\mathcal{C}_i = \{c : \|c - c_{0,i}\|_2 \leq R_i^C\}$ . The actual training and testing costs are sampled inside a slightly smaller ball of radius  $R_i = \gamma_i R_i^C$ ; after the Gaussian factor perturbation is drawn, the code radially clips it whenever necessary so that  $\|c - c_0\|_2 \leq R_i$ . Thus the known-prior data are truncated to the intended local region, while the prior set given to OURSEXACT is the larger ball of radius  $R_i^C$ . Both radii are listed in Table 1. For the Netlib cases, the same latent Gaussian factor  $\theta$  is converted into a bounded log-multiplicative perturbation of the nominal costs and is then clipped to the same local ball.

In the unknown-prior experiments the learner is not given  $\mathcal{C}_i$ . The costs are generated from the same nominal center  $c_0$  and reference radius  $R_i$  but are not radially clipped:

$$c = c_0 + U_c \theta, \quad \theta_j \sim \mathcal{N}\left(0, (\eta_i \alpha_i R_i \beta_i^{j-1})^2\right),$$

where  $\eta_i$  is an experiment-specific scale multiplier. The main unknown-prior figures use  $\eta_i = 0.35$  for Packing, MinCostFlow, and GROW7,  $\eta_i = 20$  for RandomLP A–D, and an ambient-coordinate Gaussian with  $\eta_i = 5.2$  for SC205. The  $\rho$ -sensitivity figure uses the same construction with  $\eta_i = 0.40$  for Packing,  $\eta_i = 25$  for RandomLP A/C, and an ambient-coordinate Gaussian with  $\eta_i = 50$  for SC205.

## B.1 Natural-prior benchmark

**Protocol.** The natural-prior benchmark uses packing, maxflow, mincostflow, shortest\_path, RandomLP A–D, and the Netlib instances GROW7, SC205, SCAGR25, and STAIR. In this experiment the exact learner is given the intended prior set and is denoted OURSEXACT. We compare it with RAND, DATADRIVENPROJ, FCNN-C, and FULL. RAND is a random projection baseline, DATADRIVENPROJ is the PCA-based shared projection baseline, FCNN-C is the cost-only neural projection baseline, and FULL solves the original LP and serves as the normalization reference.

In the reduced-dimension sweep, the projection baselines are evaluated at  $K \in \{5, 10, 20, 30, 40, 50\}$ . Exact compression learns its own rank from the representation sample, so its objective ratio is repeated across the displayed  $K$  values as an exact-recovery reference. In the sample-efficiency study,

Table 1: LP instances and cost-distribution parameters. Here  $d$  is the decision dimension of the LP used by the algorithms, after lossless bound normalization for Netlib MPS files,  $r_c$  is the rank of the planted cost-variation subspace,  $R_i^C$  is the radius of the known-prior ball, and  $R_i$  is the smaller radius used to sample and clip the known-prior training and testing costs. The center  $c_{0,i}$  is always reported in the same general-form cost coordinates as the displayed LP.

Instance	construction	$d$	$r_c$	$\ c_0\ _2$	coordinate range of $c_0$	$R_i^C$	$R_i$	$(\alpha, \beta)$
Packing	block packing	360	28	42.344	$[-4.069, 0]$	1.694	1.524	(0.92, 0.94)
MaxFlow	DAG max-flow	300	12	22.212	$[-3.239, 0]$	$1.28 \times 10^{-3}$	$1.15 \times 10^{-3}$	(0.95, 1.00)
MinCostFlow	unit-flow min-cost-flow	360	28	3228.138	$[-464.800, -4.960]$	3.968	3.492	(0.72, 0.94)
ShortestPath	$16 \times 16$ grid shortest path	480	16	1449.364	$[-95.000, -3.000]$	$4.72 \times 10^{-2}$	$4.49 \times 10^{-2}$	(0.70, 0.82)
RandomLP A	random bounded LP	140	24	10.763	$[-2.597, 2.634]$	$2.87 \times 10^{-3}$	$2.64 \times 10^{-3}$	(0.70, 0.82)
RandomLP B	random bounded LP	180	26	13.100	$[-2.187, 3.226]$	$8.07 \times 10^{-3}$	$7.26 \times 10^{-3}$	(0.70, 0.82)
RandomLP C	random bounded LP	220	28	14.803	$[-3.053, 2.842]$	$2.15 \times 10^{-3}$	$1.89 \times 10^{-3}$	(0.70, 0.82)
RandomLP D	random bounded LP	260	30	16.075	$[-2.350, 2.154]$	$2.40 \times 10^{-3}$	$2.06 \times 10^{-3}$	(0.70, 0.82)
GROW7	Netlib MPS	301	20	20.445	$[-7.000, 0]$	$1.26 \times 10^{-2}$	$1.16 \times 10^{-2}$	(0.70, 0.82)
SC205	Netlib MPS	203	20	1.000	$[-1.000, 0]$	$3.89 \times 10^{-4}$	$3.58 \times 10^{-4}$	(0.70, 0.82)
SCAGR25	Netlib MPS	500	24	4375.781	$[-662.000, 54.900]$	$4.80 \times 10^{-2}$	$4.42 \times 10^{-2}$	(0.70, 0.82)
STAIR	Netlib MPS	473	10	1.000	$[-1.000, 0]$	$8.14 \times 10^{-5}$	$1.63 \times 10^{-6}$	(0.70, 0.82)

$K = 20$  is fixed only for the approximate baselines, while OURSEXACT again uses the dimension discovered by Algorithm 1. The main metric is the average test objective ratio. Shaded bands show standard errors over retained random seeds.

Figure 5 shows a clear separation on the RandomLP families and on the harder Netlib instances. OURSEXACT attains full or near-full objective value across these panels, whereas DATADRIVENPROJ remains far below one on RandomLP B/D, GROW7, SCAGR25, and much of SC205. FCNN-C is often the strongest approximate baseline on RandomLP A–D and can improve at larger  $K$ , but it still falls short of exact compression except in a few large- $K$  cases.

The same benchmark also contains projection-friendly regimes. Packing, MaxFlow, ShortestPath, and STAIR are already well aligned with low-dimensional approximate projections, so most learned baselines approach the full objective there. MinCostFlow is intermediate: DATADRIVENPROJ reaches exact or near-exact behavior only after  $K$  becomes large enough, while the exact method is insensitive to this projection-budget choice because it learns the relevant directions directly.

Figure 6 highlights the sample-efficiency difference in the natural-prior setting. On RandomLP A–D, OURSEXACT quickly reaches a near-exact objective ratio as more optimal-face directions are observed, while DATADRIVENPROJ stays around a substantially lower plateau and FCNN-C improves more gradually. The same pattern appears on GROW7, where the projection baselines remain weak even as the training set grows. By contrast, Packing, MaxFlow, and ShortestPath are easy for both exact compression and the stronger approximate baselines.

Figure 7 reports the learned dimensions on the same synthetic LP instances. The graph-structured families saturate quickly, while Packing and the RandomLP instances expose larger optimal-face subspaces before stabilizing. This figure is the known-prior analogue of Figure 2.

## B.2 Additional unknown-prior diagnostics

**Protocol.** The unknown-prior experiment removes access to the true prior set. For OURSESTC, we construct a calibrated estimated prior of the form  $\hat{\mathcal{C}} = \{c : s_{\hat{\rho}}(c) \leq S_{(k)}\}$  using the ridge Mahalanobis score from Section A.3.1. Unless otherwise stated, the outside-mass parameter is  $\rho = 0.1$ . The radius is determined by calibration scores and the order statistic  $S_{(k)}$ ; no Gaussian quantile or parametric Gaussian coverage model is used. In the fixed-sample clean-split comparisons, the scripts use

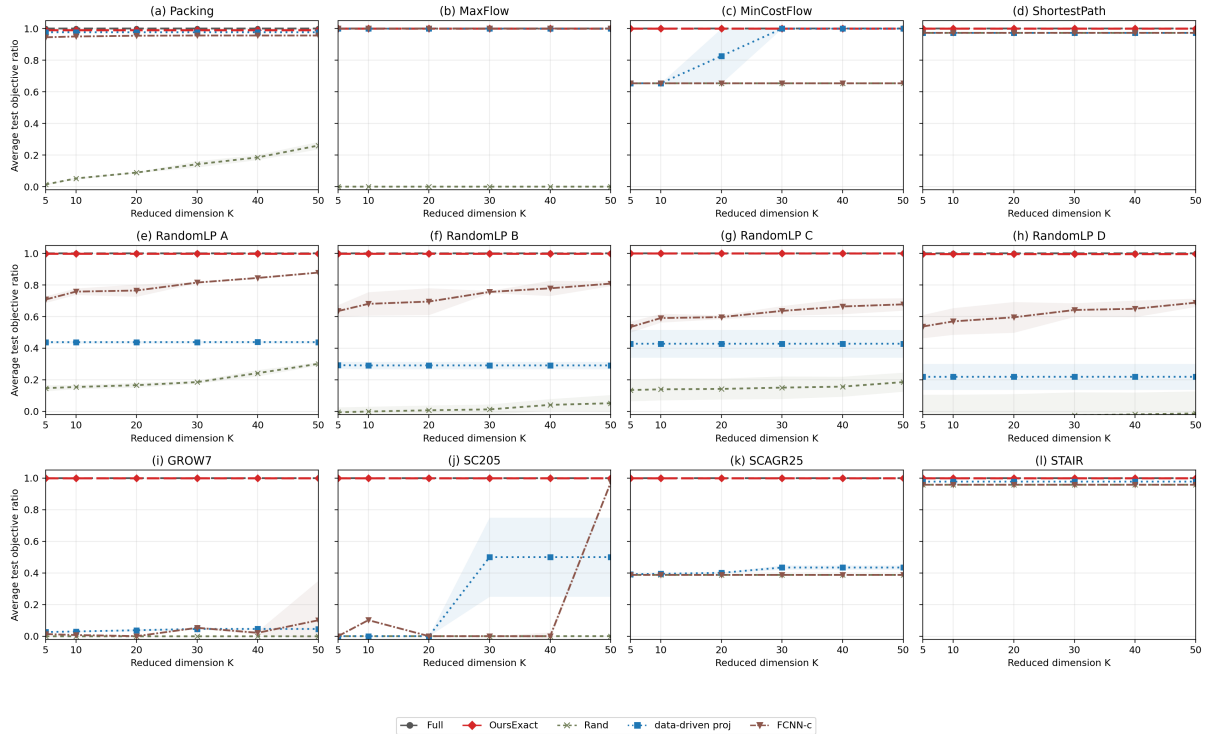


Figure 5: Objective ratio as the projection-baseline dimension  $K$  varies under natural priors. Our method is plotted as a reference across all displayed  $K$  values.

separate historical batches for fitting, calibration, and representation learning. In the sample-budget diagnostics, the horizontal axis counts the same observed costs used to fit/calibrate the working prior and to train the exact-compression learner, so OURSESTC and the projection baselines are compared at the same displayed sample budget.

The projection baselines are trained directly on the observed cost samples and do not construct an estimated prior. Thus the comparison isolates whether a calibrated convex set, followed by exact compression inside that set, is useful when the true prior is unavailable.

Figure 8 gives the broad reduced-dimension comparison under the calibrated unknown-prior protocol. OURSESTC achieves exact or near-exact performance on the retained unknown-prior test instances. The approximate baselines can be strong on projection-friendly instances such as Packing and MinCostFlow, but they remain substantially below exact compression on RandomLP B–D and GROW7. This supports the same conclusion as in the main-text: the calibrated prior is useful because it lets the exact learner focus on the high-mass region where decisions must be recovered.

Figure 9 complements Figure 4 by fixing the sample budget and varying the reduced dimension for FCNN-C. Figures 10 and 11 report the corresponding diagnostics for the PCA-based DATADRIVENPROJ baseline. The baseline is highly effective on Packing and MinCostFlow, where a shared low-dimensional projection aligns well with the observed optimizer geometry. In conclusion, our exact reduction substantially outperforms all baselines in terms of data requirement and accuracy.

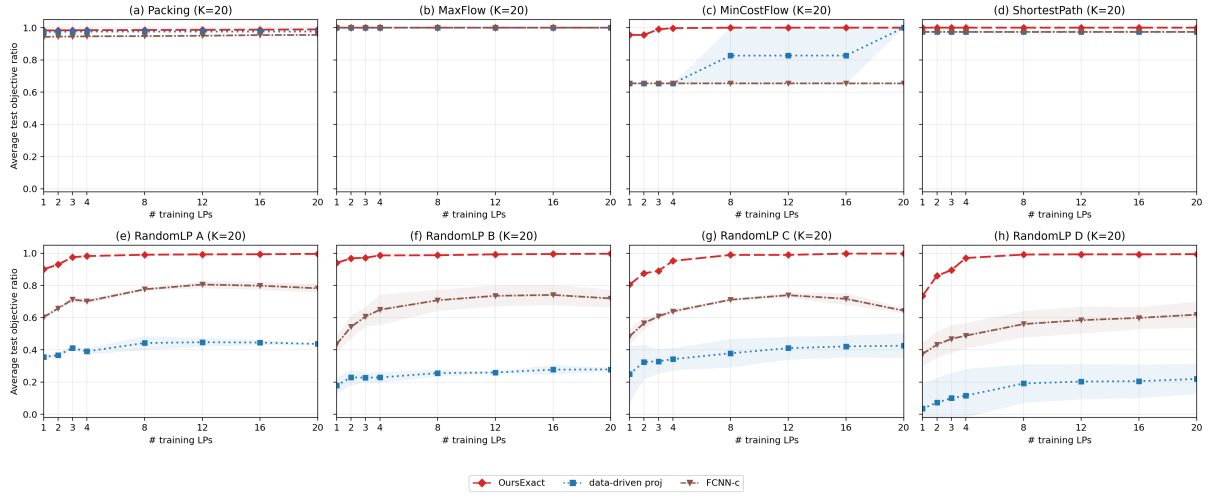


Figure 6: Objective ratio as the sample size varies under natural priors.

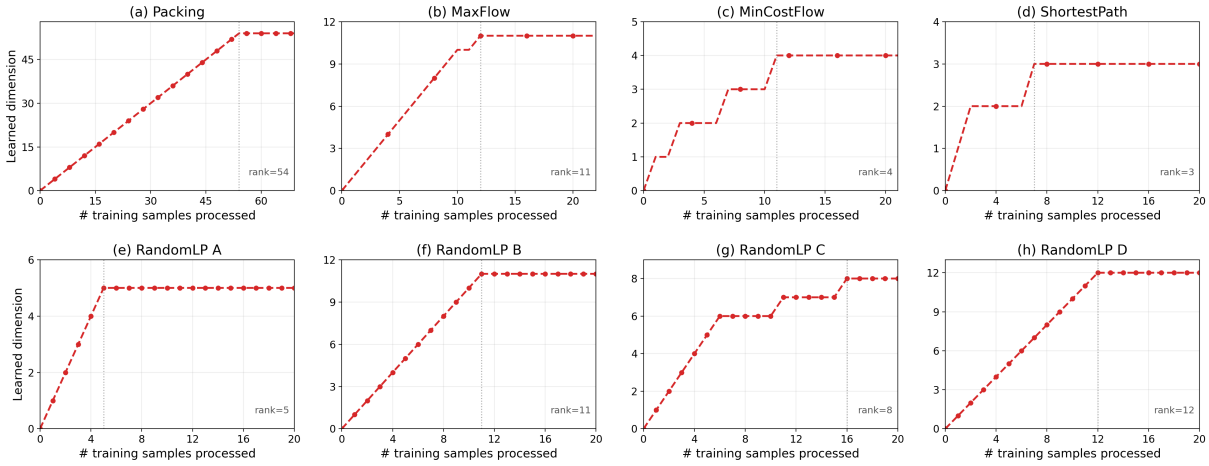


Figure 7: Learned dimension growth of our algorithm on the original synthetic LP instances.

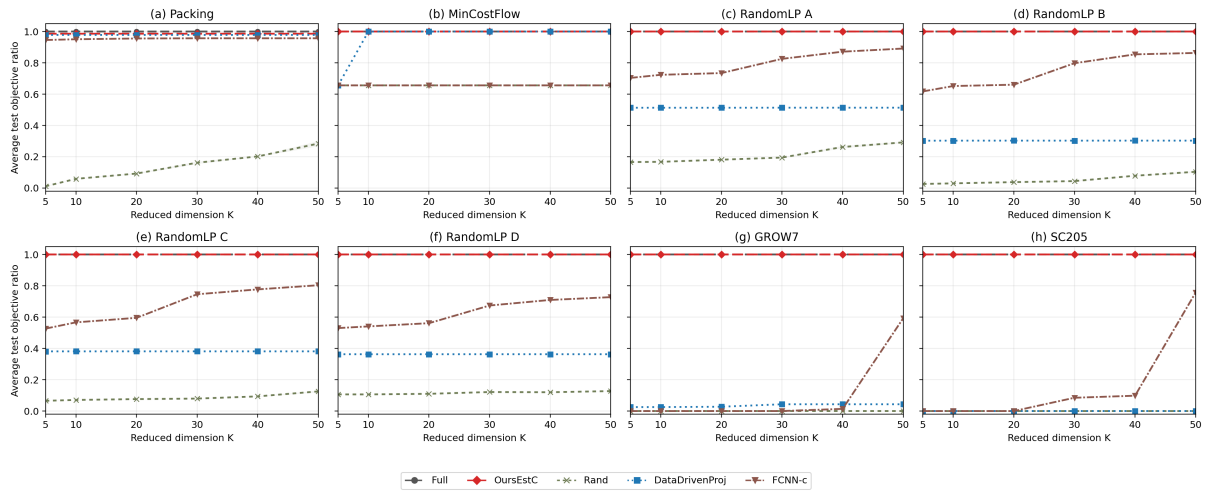


Figure 8: Reduced-dimension sweep with an unknown prior set.

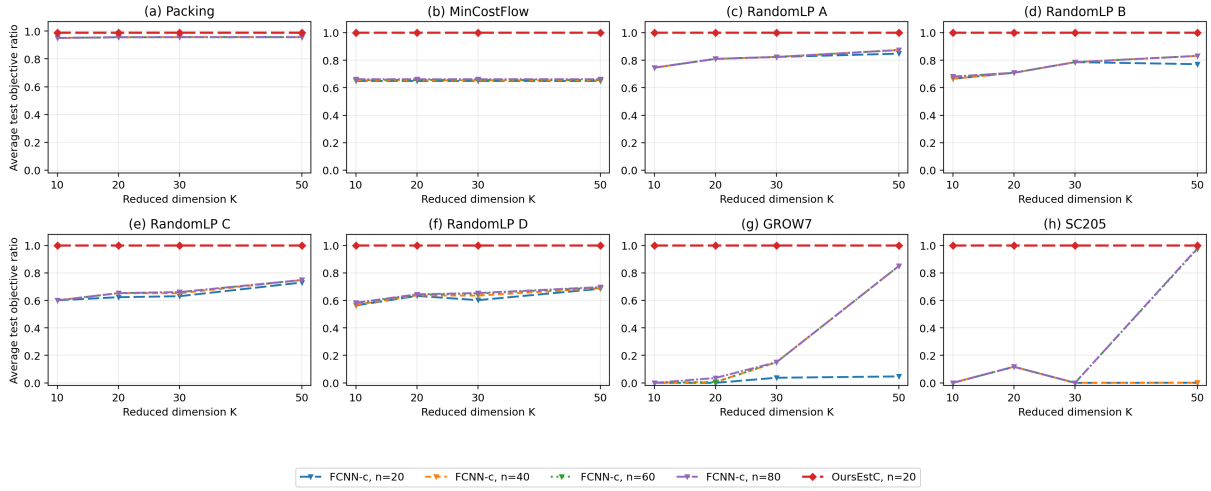


Figure 9: Reduced-dimension sweep for the plain-random FCNN-c baseline, with the  $n_{samples} = 20$  OURSESTC result shown as a reference.

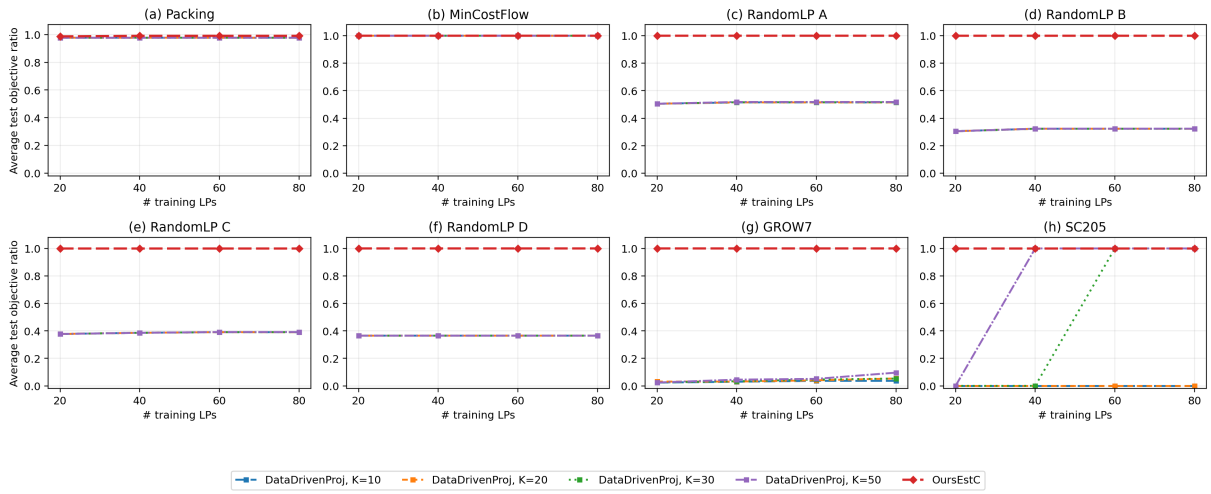


Figure 10: Sample-efficiency study for the merged DATADRIVENPROJ baseline, with OURSESTC shown as the reference.

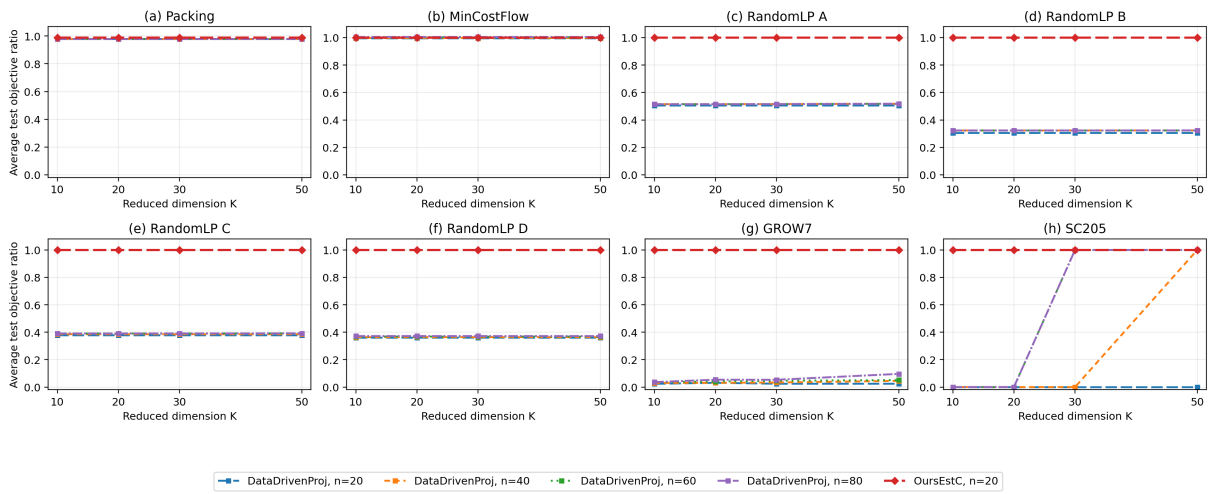


Figure 11: Reduced-dimension sweep for the DATADRVENPROJ baseline, with the  $n = 20$  OURSESTC result shown as the reference.